Genomic insights into a critically endangered island endemic songbird provide a roadmap for preventing extinction

Ross Crates[1], Brenton von Takach[1], Catherine M Young[1], Dejan Stojanovic[1], Linda Neaves[1], Liam Murphy[1], Daniel Gautschi[1], Carolyn J Hogg[1], Robert Heinsohn[1], Phil Bell[1], and Katherine A Farquharson[1]

[1]Affiliation not available

September 19, 2023

TITLE : Genomic insights into a critically endangered island endemic songbird provide a roadmap for preventing extinction.

RUNNING TITLE: King Island Scrubtit conservation genetics.

AUTHORS : Ross Crates[1¶], Brenton von Takach[2], Catherine M Young[1], Dejan Stojanovic[1], Linda Neaves[1], Liam Murphy[1], Daniel Gautschi[1], Carolyn J. Hogg[3,4], Robert Heinsohn[1], Phil Bell[5], Katherine A. Farquharson[3,4].

1. Fenner School of Environment and Society, Australian National University, Linnaeus Way, Acton, Canberra 2601.

2. School of Molecular and Life Sciences, Curtin University, Bentley, Perth, Western Australia 6102.

3. The University of Sydney, School of Life and Environmental Sciences, NSW 2006, Australia

4. Australian Research Council Centre of Excellence for Innovations in Peptide and Protein Science, The University of Sydney, NSW 2006, Australia

5. Biological Sciences, School of Natural Sciences, University of Tasmania, Hobart, Tasmania, 7005, Australia

¶Corresponding Author: ross.crates@anu.edu.au

ABSTRACT: Small, fragmented or isolated populations are at risk of population decline due to fitness costs associated with inbreeding and genetic drift. The King Island scrubtit *Acanthornis magna greeniana* is a critically endangered endemic subspecies of the nominate Tasmanian scrubtit *Acanthornis magna magna,* with an estimated population of <100 individuals persisting in three patches of swamp forest. The Tasmanian scrubtit is widespread in wet forests on mainland Tasmania. We sequenced the scrubtit genome using PacBio HiFi and undertook a population genomics study of the King Island and Tasmanian scrubtit using a double-digest restriction site-associated DNA (ddRAD) dataset of 5,239 SNP loci. The genome was 1.48 Gb long, comprising 1,518 contigs with an N50 of 7.715 Mb. King Island scrubtits formed one of four overall genetic clusters, but separated into three distinct subpopulations when analysed separately. Pairwise F_{ST} values were greater among the King Island scrubtit subpopulations than among most Tasmanian scrubtit subpopulations. Genetic diversity was lower and inbreeding coefficients were higher in the King Island scrubtit than all except one of the Tasmanian scrubtit subpopulations. We observed crown baldness in 8/15 King Island scrubtits, but 0/55 Tasmanian scrubtits. Six loci were significantly associated with baldness, including one within the DOCK11 gene which is linked to early feather development. Contemporary gene flow between King Island scrubtit subpopulations is unlikely, with further field monitoring required to quantify

the fitness consequences of its small effective size, low genetic diversity and high inbreeding. Evidence-based conservation actions can then be implemented before the taxon goes extinct.

KEY WORDS : Australia; Conservation; Evidence; Genetic rescue; Ornithology; Population Monitoring; Translocation.

1. INTRODUCTION: When populations decline and become fragmented, changes to patterns of gene flow and reductions in effective population size can exacerbate population declines through depressed individual fitness associated with inbreeding and genetic drift (Frankham 1995, Harrisson et al. 2019). Therefore, the importance of understanding the dynamics of threatened species' populations at the molecular level is increasingly being acknowledged in conservation (Allendorf et al. 2010). Without such knowledge, potentially significant drivers of population decline can be overlooked if the focus of monitoring efforts is solely at the individual or population level (Stojanovic et al. 2022). Aided by ever-improving sequencing and analytical techniques, there is little doubt that the value of population genomics to threatened species conservation will continue to increase (Willi et al. 2022).

For small, inbred populations, genetic rescue can have significant conservation benefits (Frankham et al. 2015). Meta-analysis revealed that outcrossing through the introduction of novel genes from external populations had beneficial effects on over 90% of inbred populations examined, with a median increase in composite fitness of over 145% in stressful environments (Frankham et al. 2015). Examples of successful genetic rescue include the mountain pygmy possum *Burramys parvus* , whose population more than doubled in three years following the introduction of six males from an external population (Weeks et al. 2017), and the bighorn sheep *Ovis canadensis* , whereby experimental restoration of immigration into a small inbred population led to increases in fitness-related traits of 23 – 257% (Hogg et al. 2006).

Here we address a key knowledge gap in our understanding of an Australian bird considered the third most likely to go extinct within fifteen years; the critically endangered King Island scrubtit *Acanthornis magna greeniana* (Geyle et al. 2018). King Island scrubtits are a subspecies of the nominate Tasmanian scrubtit *Acanthornis magna magna* restricted to King Island, a 1098 km^2 island within the Bass Strait between Victoria and mainland Tasmania. Expert elicitation estimated the King Island scrubtit had an 83 % probability of extinction within 20 years (95 % CI = 66 – 93 %, Geyle et al. 2018). The primary driver of King Island scrubtit population decline is habitat loss (Webb et al. 2016). While the exact habitat preferences of King Island scrubtits are not certain, surveys suggest the birds prefer swamp forest containing dominant or sub-dominant swamp paperbarks *Melaleuca ericifolia* (Webb et al., 2016; Bell et al. 2023). It is likely the King Island scrubtit would once have been widespread in suitable native vegetation prior to European colonisation $>$ 100 years ago, but extensive surveys of potentially suitable habitat fragments suggest it is now confined to three patches: Colliers Swamp in the south, Pegarah State Forest and surrounding forests in the east, and Lavinia State Reserve and a small area of private land between The Nook swamps and Granite Lagoon in the northeast (Webb et al., 2016; Bell et al. 2023, Figure 1). The total estimated area of occupancy of the King Island scrubtit is $<$ 1 km^2 and likely declining (Webb et al. 2016).

The three known putative subpopulations of the King Island scrubtit are separated by 18 to 20 km, between which lies a matrix dominated by agricultural land, sand dunes and potentially unsuitable scrub and heath vegetation types (Figure 1). The extent to which individual scrubtits can permeate the matrix and facilitate gene flow between the subpopulations is unknown, but predicted to be low based on the species' habitat preferences. Field surveys estimate the Colliers Swamp subpopulation contains approximately 30-40 birds, Pegarah Forest 15-30 birds and Nook Swamps 10-20 birds (Webb et al. 2016, Bell et al. 2023), but the effective population size of each subpopulation is unknown. There is a risk that genomic impacts associated with small effective population size and limited dispersal capacity may be contributing to the decline of the King Island scrubtit population (Frankham 2015). Other threats facing King Island scrubtits include acid sulphate soils associated with drainage for agriculture, wildfires, predation by feral cats, and habitat deterioration through windthrow and sea-level rise (Fielding et al., 2022; Webb et al., 2016). The King Island scrubtit is therefore a priority species for conservation actions under the Australian Government's Threatened Species Action

Plan 2022-32 (Commonwealth of Australia 2022).

In contrast to the King Island scrubtit, Tasmanian scrubtits are not considered threatened and are widespread in suitable habitats on mainland Tasmania and close offshore islands, though there is currently no reliable population estimate (BirdLife International 2022). The species prefers wet forest habitats which dominate the western side of mainland Tasmania but are patchier on the eastern side (Figure 1). There is no information on dispersal in Tasmanian or King Island scrubtits, though the species is understood to be largely sedentary (Higgins et al. 2006).

To assess the need for and to inform potential genetic management of the King Island scrubtit, our study had four aims: firstly to sequence the scrubtit genome; second to estimate the current spatial genetic structure of the King Island scrubtit population; third to quantify current levels of genetic diversity, inbreeding and relatedness within the King Island scrubtit population; and finally to consider the population genetics of the King Island scrubtit within the context of the genetics of the Tasmanian scrubtit. Following population genetic theory and available demographic data (Frankham 1995; Webb et al. 2016), we predicted that, relative to the Tasmanian scrubtit, the King Island scrubtit population would have higher levels of population structure and inbreeding and lower genetic diversity.

2. MATERIALS AND METHODS:

2.1 Sample collection

To obtain indicative genetic diversity metrics across mainland Tasmania, we sampled between five and eleven scrubtits from seven *a-priori*subpopulations on mainland Tasmania (including Bruny Island) during the non-breeding season (January – March 2021). Due to small population sizes and licensing restrictions on King Island, we sampled five individuals from three locations during the same non-breeding season (Table 1, Figure 1). We trapped scrubtits using a single 6m mist net and one minute of scrubtit song broadcast using portable speakers (ANU animal ethics permit # A2021/33). We sampled blood ($<$ 20 µl per individual) using the standard brachial venepuncture technique with a 0.7mm needle into 70% ethanol. For two individuals from whom we were unable to safely obtain blood, we collected feathers shed during handling. One male individual was collected under licence (see acknowledgements) for genome sequencing, from which organ tissue samples (heart, spleen, kidney, gonads, brain, liver) were taken (Table S1). For each individual we took standard morphometric measurements and scanned for any unusual physical features such as feather abnormalities or skin lesions that may be indicators of poor health. A single observer (CY) sampled and measured all birds, and the maximum capture time was 35 minutes. No birds showed adverse reactions to sampling and all flew off strongly upon release. The fifteen individuals sampled on King Island was the maximum permissible sample size under licence conditions.

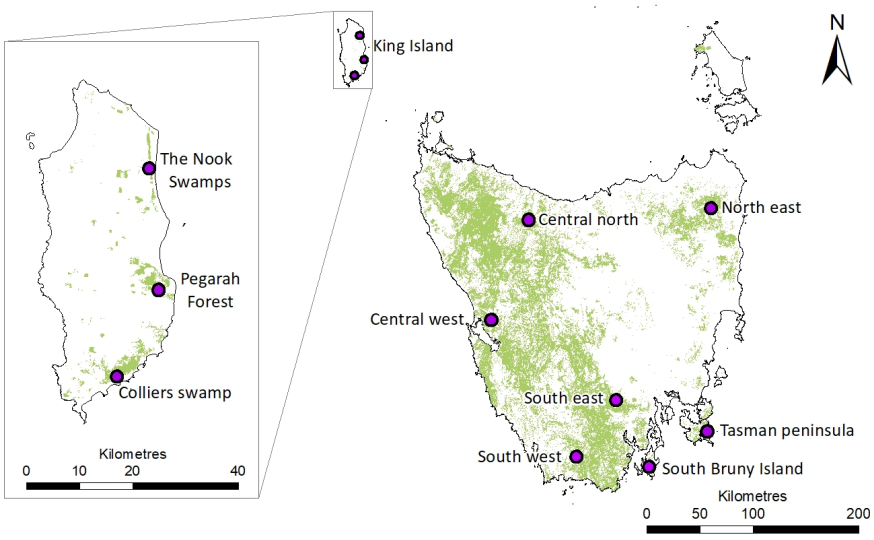

Figure 1: Sampling locations of Tasmanian scrubtit (right) and King Island scrubtit (left). Shown in green is the distribution of wet eucalypt forest, swamp forest and rainforest. Vegetation data are derived from TASVEG v4.0.

2.2 DNA extraction, sexing and sequencing

High molecular weight DNA was extracted from flash frozen heart and kidney using the Nanobind Tissue Big DNA Kit v1.0 11/19 (Circulomics). A Qubit fluorometer was used to quantify DNA concentrations with the Qubit dsDNA BR assay kit (Thermo Fisher Scientific). RNA was extracted from heart, spleen, kidney, gonads, brain, and liver stored in RNA later using the RNeasy Plus mini Kit (Qiagen) with RNAse-free DNAse (Qiagen) digestion. RNA quality was assessed via Nanodrop (Thermo Fisher Scientific). We extracted DNA for population genomics from blood and feather samples using the Monarch® Genomic DNA Purification Kit (New England BioLabs, Victoria, Australia). We quantified DNA concentrations using a Qubit 3.0 fluorometer (yield range 10.3 – 209 ng μl^{-1}, Table S1) and standardised the concentration of each sample to 10-30 ng μl^{-1} DNA for 20-25 µl and determined the sex of individuals using a polymerase chain reaction (PCR) protocol adapted from Fridolfsson and Ellegren (1999, Supplementary file S1). We arranged the samples on a single 96 well plate, containing five technical replicates of the samples with the highest DNA concentrations, an additional 21 non-technical replicates including all of the King Island samples, five extra samples from mainland Tasmania and one negative control.

Double-digest restriction associated DNA (ddRAD) sequencing following Peterson et al. (2012) was undertaken at the Australian Genome Research Facility, Melbourne on an Illumina NovaSeq 6000 platform using 150bp paired-end reads. Samples were first quantified using Quantifluor and visualised on 1 % agarose e-gel to ensure all samples exceeded the minimum input DNA quantity of 50 ng. Three establishment samples with at least 250 ng DNA that were representative of the distribution of the samples (2 Tasmanian scrubtits, 1 King Island scrubtit) were used to determine the optimal combination of restriction enzymes, which were *EcoRI* and *HpyCH4IV* . Further details on the library preparation protocol are provided in Supplementary file S1.

2.3 Genome sequencing and assembly

Full methodological details of the genome and transcriptome sequencing and assembly are provided in Supplementary file S2. In summary, high molecular weight DNA was sent for PacBio HiFi library preparation with Pippin Prep and sequencing on one single molecule real-time (SMRT) cell of the PacBio Sequel II (Australian Genome Research Facility, Brisbane, Australia). Total RNA was sequenced as 100 bp paired-end reads using Illumina NovaSeq 6000 with Illumina Stranded mRNA library preparation at the Ramaciotti

Centre for Genomics (University of New South Wales, Sydney, Australia). Genome assembly was conducted on Galaxy Australia (The Galaxy Community, 2022) following the genome assembly guide (Price & Farquharson, 2022) using HiFiasm v0.16.1 with default parameters (Cheng et al., 2021; Cheng et al., 2022). Transcriptome assembly was conducted on the University of Sydney High Performance Computer, Artemis. Genome annotation was performed using FGENESH++ v7.2.2 (Softberry; (Solovyev et al., 2006)) on a Pawsey Supercomputing Centre Nimbus cloud machine (256 GB RAM, 64 vCPU, 3 TB storage) using the longest open reading frame predicted from the global transcriptome, non-mammalian settings, and optimised parameters supplied with the *Corvus brachyrhynchos* (American crow) gene-finding matrix. The mitochondrial genome was assembled using MitoHifi v3 (Uliano-Silva et al., 2023). Benchmarking universal single copy orthologs (BUSCO) was used to assess genome, transcriptome and annotation completeness (Manni et al., 2021).

2.4 Bioinformatics pipeline and SNP filtering

Raw sequence data were processed using Stacks v2.62 (Catchen et al., 2013) and aligned to the genome with BWA v0.7.17-r1188 (Li & Durbin, 2009). Full details of the bioinformatics pipeline, which produced a variant call format (VCF) file containing 45,488 variants for SNP filtering in R v4.0.3 (R Core team 2020) are provided in Supplementary file S1. We filtered genotyped variants using the "SNPfiltR" v1.0.0 package (DeRaad, 2022) based on (i) minimum read depth ([?] 5), (ii) genotype quality ([?] 20), (iii) maximum read depth ([?] 137), and (iv) allele balance ratio (0.2 – 0.8). Then, using a custom R script, we filtered SNPs based on (i) the level of missing data (< 5%); (ii) minor allele count (MAC [?] 3), (iii) observed heterozygosity (< 0.6), and (iv) linkage disequilibrium (correlation < 0.5 among loci within 500,000 bp).

To ensure that relationships between individuals could be accurately inferred from the data, we used these SNPs and samples to construct a hierarchical clustering dendrogram based on genetic distance, with visual examination of the dendrogram confirming that all 24 replicates paired closely together on long branches (Figure S1). We also made a higher-level bootstrapped dendrogram by using genetic distances among sampling localities instead of individuals (Figure S2). The percentage difference between called genotypes of technical replicates was also used to confirm that genotyping error rates were low after filtering (mean 99.91% ± 0.005% SE similarity between replicates). We therefore removed one of each replicate pair from all further analyses.

We used "tess3r" (Caye et al. 2016, 2018) to perform a genome scan for loci under selection, using the Bejamini-Hochberg algorithm (Benjamini & Hochberg, 1995), with a false discovery rate of 1 in 10,000 to correct for issues associated with multiple testing. Because this method identified zero candidate loci under selection, we also used the *gl.outflank* function in "dartR" v2.0.4 to implement the OutFLANK method (Whitlock & Letterhos 2015) to infer the distribution of F_{ST} for loci unlikely to be strongly affected by spatially diversifying selection. This method also identified zero putatively adaptive loci, leaving a final dataset for formal population genetic analysis containing all 70 originally sampled individuals, 5,239 biallelic SNPs, and an overall missing data level of 0.98 %. The number of SNPs and samples removed from the dataset at each filtering step is provided in Table S2.

2.5 Statistical analysis

2.5.1 Population genomic structure

We used "poppr" v2.9.3 (Kamvar 2023) to produce a multidimensional scaling (MDS) plot of all individuals based on a matrix of Prevosti's genetic distances. To focus in more detail on the King Island population, we then repeated the MDS analysis using only the 15 individuals sampled from King Island. We then created a pairwise Weir and Cockerham (1984) fixation index (F_{ST}) matrix in "StAMPP" v1.6.3 (Pembleton 2013) with 999 bootstraps to assess significance of the estimated differentiation between populations. To assess isolation by distance at the individual level, we fitted a linear model of all standardised pairwise F_{ST} values against the geographic distance between samples (Rousset, 1997).

We used the alternating projected least squares algorithm implemented in "tess3r" to assign individuals

to ancestral population genomic clusters, investigate patterns of admixture between populations and assess hierarchical population structure. This method applies a model of genetic structure featuring a number of ancestral populations (k), allowing assessment of values for k that have low cross-entropy metrics (Frichot et al., 2014; Frichot & François, 2015). It also incorporates the spatial location of sampling, to remove potential bias associated with isolation-by-distance. We calculated cross-entropy criteria for values of k between 1 and 15, and visualised a cross-entropy scree-plot to identify a plateau or substantial change in curvature in the plot. We then extracted the matrices of individual admixture coefficients for the most relevant values of k for inference and plotted these as stacked bar plots to visualize hierarchical population structure. We then interpolated several values of k (2–4) across the landscape within the range of the scrubtit, based on the geographical location of samples. We then repeated this analysis using only the King Island scrubtit data for values of k from 1 to 5.

2.5.2 Genetic diversity, inbreeding and mean kinship

We used the *genetic_diversity* function within the "gstudio" package v1.5.3 (Dyer 2021) to calculate mean ($\pm$ standard error and standard deviation) genetic diversity metrics across the 10 subpopulations. These metrics included the number of alleles (A), effective number of alleles (A_E), observed heterozygosity (H_O), expected heterozygosity (H_E). We used the standard correction for small sample size to account for potential biases in the estimates of H_E due to variation in the number of samples obtained from subpopulations. We used "diveRsity" v1.9.90 (Keenan et al. 2013) to calculate subpopulation-level Wright's inbreeding coefficients (F_{IS}) values with confidence intervals via 1000 bootstraps. We then used "PopGenReport" v3.0.7 (Gruber & Adamack 2022) to calculate mean allelic richness (A_R) in the subpopulations and "poppr" to calculate (i) mean private alleles within all subpopulations bootstrapped to sample size of 5; and (ii) the number of private alleles only within subpopulations of the King Island scrubtit. Finally, we calculated individual inbreeding coefficients (II_C) using the 'mom.weir' method with the*snpgdsIndInbCoef* function in "SNPRelate" (Zheng et al. 2012). This method uses a modified Visscher's estimator (Yang et al. 2010).

We calculated relatedness using COANCESTRY (Wang, 2011), firstly only within the King Island subpopulations, and then within all 10 subpopulations together (King Island and mainland Tasmania). We first ran simulations as per Hogg et al (2019) to determine the best moment estimator to use. This was the triadic likelihood method (TrioML), as it weights loci relative to the number of alleles and accounts for genotyping error and inbreeding (Wang, 2007). Results are presented as mean kinship values (MK), calculated by dividing the TrioML value by 2.

2.5.3 Genetic relationship with crown baldness

During sampling, we noted that eight King Island scrubtits had a distinct bald patch on the crown of their heads (Figure S3), so explored the possibility that this feature was linked to genome-wide heterozygosity or particular SNP loci in these individuals. We used "inbreedR" v 0.3.3 (Stoffel et al. 2016) to calculate multilocus heterozygosity (MLH) values for each individual, then implemented a heterozygosity-fitness correlation analysis using logistic regression via package "lme4" v1.1-31 (Bates et al. 2015) with a binomial response of bald or not bald against (i) the entire scrubtit sample; and (ii) only King Island scrubtits. We included genotypic sex as a random term in both models.

To determine if any loci were significantly associated with baldness, we used a latent factor mixed modelling (LFMM) approach. This method tests the explanatory significance of a trait variable on the genotypic matrix, allowing for inference regarding the genetic basis of the trait. As LFMM requires no missing data, we imputed missing genotypes via the 'impute' function of the "LEA" package (Frichot & François, 2015), utilising four ancestral populations and method = "mode". We then used the 'lfmm2' exact least-squares function of the LEA package to build the LFMM object and identified allele frequencies that were correlated with each of the environmental variables (Caye et al., 2019). This method controls for population structure via a number of latent factors equal to the number of ancestral populations. We adjusted the p -values for each SNP using the robust estimate of the genomic inflation factor (Martins et al., 2016) and a Benjamini-Hochberg algorithmic correction (Benjamini & Hochberg, 1995) to ensure a low rate of false discovery (corrected to

1 in 10,000 SNPs). We then produced a Manhattan plot along with the positions of candidate SNPs. We identified the genomic coordinates of the candidate SNPs in the transcriptome-guided genome annotation to determine if they were genic or non-genic and the putative function of the gene or nearest candidate gene. If the gene was not annotated by FGENESH++, we queried the protein sequence against the National Center for Biotechnology Information (NCBI)'s RefSeq non-redundant protein sequences database using the BLASTp webserver for homology to known genes (Johnson et al., 2008).

2.5.4 Effective population size estimation

We used NeEstimator v.2 (Do et al. 2014) via the "dartR" wrapper to estimate the current effective sizes of the King Island and Tasmanian scrubtit populations as well as the subpopulations therein (Supplementary file S1).

3. RESULTS

3.1 Genome sequencing and assembly

The genome assembly was 1.48 Gb in length, comprising 1,516 contigs with a contig N50 of 7.715 Mb (Tables S3-S4). Over 99.99% of raw reads were retained after quality trimming. The genome had 97.18% complete BUSCOs [Single copy: 96.4%; Duplicated: 0.7%], 0.5% fragmented BUSCOs and 2.4% missing BUSCOs. A total of 12,877 predicted genes were used as evidence for genome annotation from the global transcriptome, which had 94.9% complete BUSCOs [Single copy: 15.0%; Duplicated: 79.9%], 1.3% fragmented BUSCOs and 3.8% missing BUSCOs. After annotation, 30,347 genes were predicted, with an annotation completeness of 82.8% BUSCOs [Single copy: 82.1%; Duplicated: 0.7%], 7.7% fragmented BUSCOs and 9.5% missing BUSCOs. The mitochondrial genome was 16,867 bp in length and was identified on a single contig (Figure S4).

3.2 Population genetic structure

The MDS plots showed evidence of four distinct genetic clusters in the scrubtit (Figure 2a). Within mainland Tasmania, individuals sampled in the northeast of the state and on the Tasman Peninsula were distinct from the rest of the mainland population. King Island scrubtits formed their own cluster distinct from the Tasmanian scrubtit, with additional substructuring into three subpopulations when analysed independently (Figure 2b).

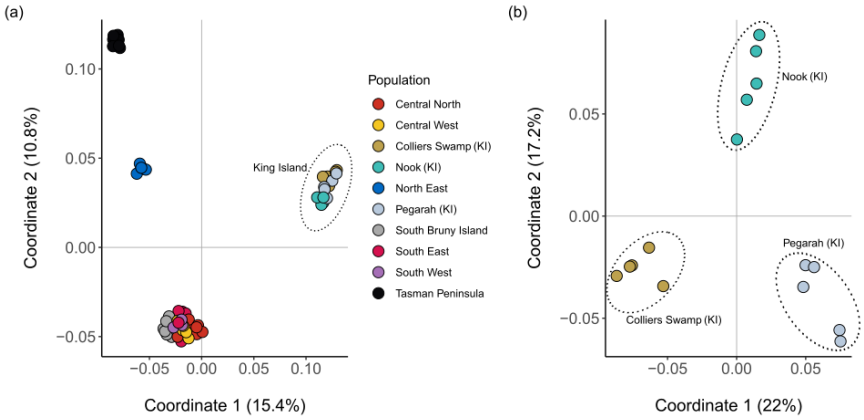

Figure 2: Multidimensional scaling plot (MDS) showing the genetic structure of scrubtit samples by population based on Prevosti's genetic distance. (a) shows all sampled individuals across mainland Tasmania and King Island; (b) shows only King Island samples. Numbers in parentheses on axis titles denote the proportion of total variance explained by the first two coordinates.

Pairwise F_{ST} estimates between the King Island subpopulations (0.12 - 0.18) were larger than the majority of the pairwise estimates between the mainland subpopulations (0.01 – 0.18) except the Tasman Peninsula (> 0.22, Table S5). Genetic isolation was positively correlated with geographic distance (glm $\beta = 494.7$, se = 101.7, $p < .001$, McFadden's $R^2 = 0.36$, Figure S5).

Increasing values of k resulted in decreased values of the cross-entropy criterion (Figure S6), with changes in the criterion value suggesting that the best number of ancestral populations for interpretation within the current sampling design ranged from 2 to 4. Admixture plots showed strong differentiation of the King Island subspecies from the Tasmanian scrubtit regardless of the estimated number of ancestral populations (Figures 3 & S7). When $k = 3$, the east coast subpopulations in the Tasman Peninsula and north east separated with a high degree of confidence from the remainder of the Tasmanian scrubtit population, and when $k = 4$ the Tasman Peninsula and north east subpopulations separated from each other. Despite being isolated from the mainland by a 4 km wide sea strait, the Bruny Island subpopulation was less isolated from the rest of the Tasmanian scrubtit population than were the north-eastern and Tasman Peninsula subpopulations (Figures 3 & S7, Table S5). When analysed independently, King Island scrubtits showed a high degree of differentiation by subpopulation when $k = 3$ (Figures 4, S8 – S9).

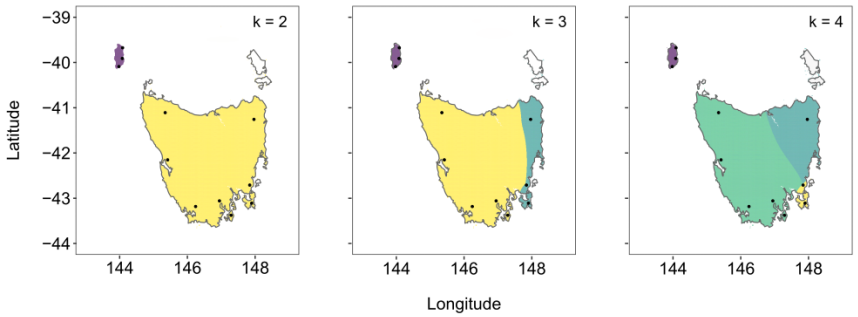

Figure 3: Patterns of landscape genomic structure across the geographical range of the scrubtit. Each panel shows the population genomic structure when two, three or four ancestral clusters ($k$values) are identified in the data. Colours in each panel represent the distribution of an ancestral cluster, interpolated across the distribution of the species. Black points indicate sampling locations.

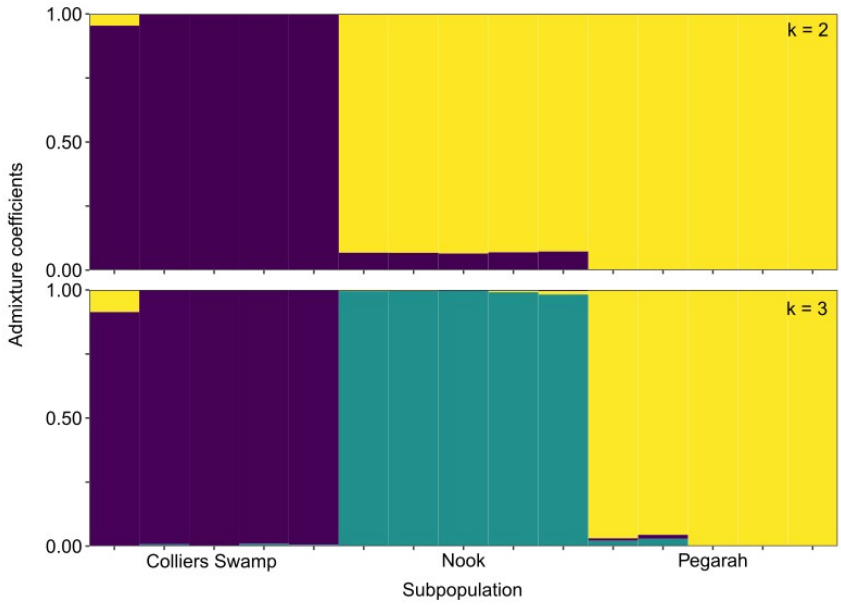

Figure 4: Admixture plots showing the probability of assignment of individual King Island scrubtits to *a-priori* subpopulations based on sampling locations when the number of ancestral populations (k) ranged from 2 to 3.

3.2 Genetic diversity, inbreeding and mean kinship

Measures of the mean number of alleles, effective number of alleles, expected and observed heterozygosity and allelic richness were all lower in the three King Island scrubtit subpopulations than they were within all of the Tasmanian scrubtit subpopulations, except the Tasman Peninsula (Table 1, Figure S10). F_{IS} confidence intervals overlapped zero in all subpopulations (Figure S10). Mean individual level inbreeding coefficients calculated using the modified Visscher's method were higher in the three King Island scrubtit populations than all of the Tasmanian scrubtit populations, again except the Tasman Peninsula (Figure 5a). The majority of King Island scrubtits plotted towards the higher end of individual inbreeding estimates across the entire sample (Figure 5b). The mean number of private alleles within the King Island scrubtit subpopulations were within the range of those of the Tasmanian scrubtit, but the number increased three-to-sixfold when King Island scrubtits were analysed separately (Table 1). Within population mean kinships for the King Island populations when analysed as the island populations only, reflected on average a first cousin relationship (˜0.0625; Table 1). However, when within population mean kinships for King Island populations were analysed with all the Tasmanian mainland populations, the within populations mean kinship for the King Island populations reflected on average a full-sibling relationship/parent-offspring (˜0.2500; Table 1). Samples from the Tasman Peninsula also reflected a mean kinship of a full-sibling/parent-offspring relationship, whilst the North East and South Bruny Island samples reflect a mean kinship of a half-sibling relationship (Table 1).

Table 1: Sample sizes by molecular sex (F/M) and population genetic parameters for the King Island and Tasmanian scrubtit. Parameters shown are number of alleles (A), number of effective alleles (A_E), SNP expected heterozygosity (H_E), SNP observed heterozygosity (H_O), Wright's inbreeding coefficient (F_{IS} $\pm$ 95 % CI), mean individual inbreeding coefficient (II_C), allelic richness (A_R), mean private alleles (PA) and within population mean kinship (mean $\pm$ SE) for King Island populations only, and for all subpopulations. See Table S6 for estimates with standard errors.

Region	Subpopulation	#F	#M*	A	A_E	H_E	H_O	F_{IS}	II_C	A_R	P_A**	M
King Island	Colliers Swamp	1	4	1.423	1.258	0.169	0.17	-0.101	0.321	1.343	45.69 (215)	0.
	Nook	2	3	1.489	1.302	0.197	0.2	-0.119	0.234	1.401	39.28 (383)	0.
	Pegarah	2	3	1.448	1.277	0.181	0.166	-0.005	0.349	1.367	46.77 (252)	0.
Mainland	Central North	3	7	1.816	1.449	0.282	0.27	0.006	0.087	1.597	41.33	
	Central West	3	3	1.753	1.439	0.284	0.27	-0.029	0.084	1.588	32.99	
	North East	3	4	1.616	1.343	0.22	0.216	-0.053	0.192	1.462	39.05	
	South Bruny Island	3	4	1.671	1.394	0.251	0.243	-0.041	0.169	1.521	84.16	
	South East	2	9	1.838	1.449	0.282	0.27	-0.006	0.077	1.601	57.85	
	South West	2	3	1.713	1.426	0.28	0.268	-0.061	0.082	1.572	29.09	
	Tasman Peninsula	3	5	1.448	1.266	0.167	0.163	-0.043	0.346	1.346	65.79	

*1 additional male collected from Weilangta for genome sequencing.

**Numbers in parentheses denote number of private alleles within the King Island subpopulations when analysed separately.

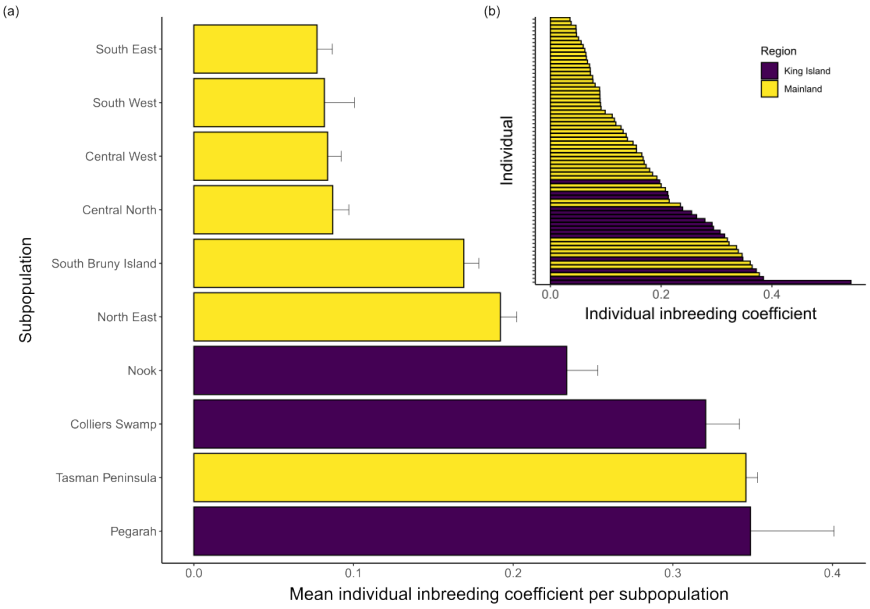

Figure 5: Inbreeding coefficients for King Island and Tasmanian scrubtits. Shown are (a) averages (± standard error) across subpopulations and (b) estimates for all individuals.

3.3. Genetic relationship with baldness

Crown baldness was present in 8/15 King Island scrubtits, including in both sexes and all three subpopulations, but none of 55 Tasmanian scrubtits. Logistic regression across all genotyped individuals showed a weak negative relationship between multi-locus heterozygosity (MLH) and the probability of crown baldness occurrence (β = -22.152. se = 8.788, z = -2.52, p = 0.017, Figure 6a). However, this relationship disappeared when the analysis was restricted to only King Island scrubtits (β = 11.56, se = 21.8, z = 0.53, p = 0.60, Figure 6b), suggesting baldness is more likely to occur in the King Island scrubtit population than the Tasmanian scrubtit population, but baldness in King Island scrubtits is not linked to (relatively) low genome-wide MLH.

After accounting for population structure ($k = 3$) and adjusting the p -values, the LFMM identified six loci that were significantly associated with baldness (Figure S11). Of the six candidate SNPs, three were genic and three were non-genic (Table S7). Three SNPs were located on the same assembled contig, including one in the *DOCK11* gene involved in regulation of filopodium assembly. Filopodia have been implicated in feather follicle formation and feather branching in chickens (Cheng et al., 2018), suggesting a possible role of this gene in baldness.

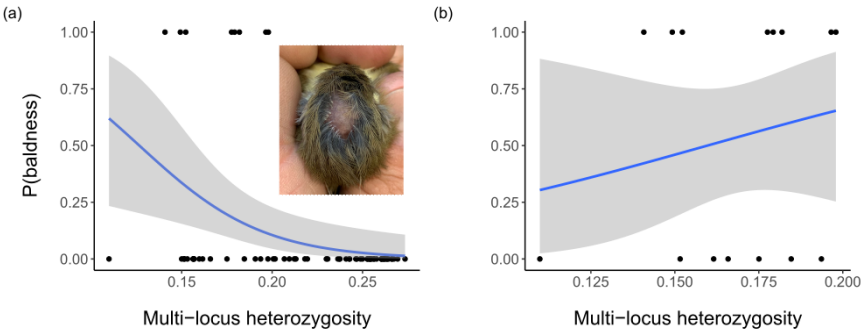

Figure 6: Logistic regression plots showing the relationship between multi-locus heterozygosity and probability of crown baldness in (a) all scrubtit samples and (b) King Island scrubtits. Inset image within (a) shows example of King Island scrubtit with crown baldness.

3.4 Effective population size estimation

At $k = 3$, NeEstimator calculated small effective population sizes on King Island and the east coast of the mainland ($N_e$for both populations < 20), but also calculated a relatively small effective population size for the remainder of the mainland ($N_e = 137$, Table S8). We suggest these results be interpreted with caution as N_e values can be difficult to accurately estimate with ddRAD data.

DISCUSSION

We explored the population genomic status of the critically endangered King Island scrubtit in the context of its mainland congener - the Tasmanian scrubtit, using a genome-wide SNP dataset developed with samples collected from across their contemporary distribution. We also provide the first sequenced and assembled long-read genome for the family *Acanthizidae.* We show that the scrubtit population is structured into four genetic clusters, with additional substructuring of the King Island scrubtit population when analysed independently. Genomic diversity is lower and inbreeding coefficients are higher in the King Island scrubtit than in the Tasmanian scrubtit. Crown baldness was present in over 50% of King Island scrubtits, but none of the 55 Tasmanian scrubtits. Baldness was not linked to particularly low levels of multi-locus heterozygosity in King Island scrubtits, but was significantly associated with six candidate SNPs. Below, we discuss the implications of these results for research and genetic management requirements of the King Island scrubtit.

Population genomic structure

The patterns of population genomic structure in scrubtits add further evidence that Tasmanian biodiversity is broadly structured by biogeographic barriers related to climate, topology and anthropogenic impacts. King Island scrubtits likely diverged from Tasmanian scrubtits towards the end of the Pleistocene glacial period around 12,000 years ago, when sea level rise flooded low-lying marshlands in what is now the Bass Strait (Bowdler 2015). King Island scrubtits are therefore already occupying a climate refuge, and habitat loss following European settlement has fragmented this refuge into three isolated subpopulations. Our results suggest these subpopulations are now unlikely to be connected by natural gene flow, with genetic differentiation between the subpopulations resulting from vicariance and genetic drift. Pairwise F_{ST} values between King Island subpopulations are similar to or greater than those between Tasmanian scrubtit subpopulations,

despite the substantially smaller geographic distances between those on King Island (circa 20 km) than those on the Tasmanian mainland (60 – 100 km). This suggests that the nature of the matrix surrounding the King Island subpopulations is more of a barrier to dispersal than the distances between them.

Among Tasmanian scrubtits, east coast birds are isolated somewhat from the rest of the population by a broad swathe of unsuitable habitats associated with a warmer and drier climate in the midlands (Corney et al. 2013), comprising predominantly dry sclerophyll forest that has also been heavily cleared since European arrival (Figure 1). The distribution of wet sclerophyll forest and rainforest within the east coast is patchy. Tasman Peninsula scrubtits are isolated by ocean on three sides and a narrow neck of land on the fourth, but dispersal is likely also limited by a lack of wet forest and land clearing on the nearby mainland (Figure 1). This pattern of genetic isolation of the Tasman Peninsula scrubtit is similar to the patterns observed in other taxa including the Tasmanian devil *Sarcophilus harrisii* (Jones et al. 2004; Farquharson et al. 2022) and mountain ash *Eucalyptus regnans* (von Takach et al. 2021). In contrast, wet forest is abundant on the mainland adjacent to south Bruny Island. This suggests occasional gene flow across the 4 km strait separating Bruny Island from the Tasmanian mainland can occur, as has been demonstrated in forty-spotted pardalotes*Pardalotus quadragintus* (Alves et al. 2023).

Genetic diversity, inbreeding and mean kinship

Consistent with our predictions, observed levels of genetic diversity were significantly lower in King Island scrubits than in all Tasmanian scrubtit subpopulations apart from the Tasman Peninsula. Interestingly, the samples from the Tasman Peninsula exhibit the similar within-population mean kinship values as those on King Island. Relatively lower levels of genomic diversity are observed in many island vertebrate populations, particularly on small islands as shown in northern quolls *Dasyurus hallucatus* (von Takach et al. 2022) and black-footed tree rats (Djintamoonga) *Mesembriomys gouldii* (von Takach et al. 2023). Individual inbreeding coefficients and mean kinship measures were also higher in the King Island scrubtit than in the Tasmanian scrubtit but, against our predictions, inbreeding measures (F_{IS}) were lower for the Colliers Swamp and Nook Swamps subpopulations than for all Tasmanian scrubtit subpopulations. F_{IS} detects non-random mating in the most recent generation (Waples, 2015), so our lower-than-expected estimates for these two King Island subpopulations could simply mean that these individuals are not mating with close relatives. However, other results — notably the reasonably high individual inbreeding coefficients calculated from the modified Visscher's method (Figure 5) — suggest these unusually low F_{IS} values may be explained by small and / or sex-biased sampling and therefore requires further study.

Phenotypic evidence of defective traits in small, inbred populations is likely to occur but not always noticed in wild systems (but see e.g. Roelke et al. 1993 and Harrisson et al. 2019). Although unknown at this time if it is a defective trait or not, over 50 % of King Island scrubtits we sampled exhibited crown baldness (Figures 5 & S3). Baldness was present in both sexes and all three King Island subpopulations, but was not recorded in any Tasmanian scrubtits. The probability of baldness was negatively associated with multi-locus heterozygosity, but the relationship disappeared when we restricted the analysis to the King Island population. It is possible that baldness may be due to non-genetic effects such as endemic parasitism, disease, inter/intraspecific aggression linked to low habitat availability or an ageing population (Lachish et al. 2012; Thys et al. 2017; van Velden et al. 2017). However, baldness was similar in all affected individuals (Figure S3) and we found six candidate SNPs that may play a role in the development or expression of this trait. One of these SNPs is associated with the DOCK11 gene, a gene that has been linked to early feather development in chickens (Figure S10; Table S7; Cheng et al. 2018). Further investigation into the phenotype-genotype associations may be able to determine the genetic and physiological pathways leading to baldness.

Conservation implications

The principal threat to persistence of the King Island scrubtit is habitat loss and its small population size (Threatened Species Section, 2012). Preservation of remaining habitat and restoration of lost habitat will therefore be critical if the taxon is to recover in the longer term (Webb et al. 2016). In the shorter term, our results suggest the Pegarah Forest, Colliers Swamp and Nook Swamps subpopulations of the King Island

scrubtit should be managed as a single management unit with translocations between these small, isolated populations used to improve gene flow that has been lost due to habitat fragmentation and ensure that the current level of overall genetic diversity is maintained (Frankham et al 2017). Higher levels of inbreeding, lower estimated effective population sizes and higher probability of visible defective traits (i.e. baldness) relative to the Tasmanian scrubtit suggest that genetic factors may well be exacerbating population decline in King Island scrubtits. Future genetic management of the population is therefore warranted. There are currently no demographic data on dispersal and breeding success rates in King Island scrubtits. However, if breeding success is low and / or contemporary gene flow between subpopulations is as infrequent as our results suggest, genetic rescue through the translocation of scrubtits between King Island subpopulations could help (Harrisson et al. 2016).

Action paralysis is a conscious management decision when threats are known, and risks of adverse events may be worth taking if a species or population is already known to be on a course for imminent extinction (Webb et al. 2018, Canessa et al. 2020). For many years, the risk of outbreeding depression has been used as an excuse for inaction (Ralls et al. 2018), however evidence for outbreeding depression is limited and predictable (Frankham et al. 2011, Frankham 2015). A very real risk of any translocation is that introduced individuals may be vectors for the establishment of novel pathogens in threatened populations (Peters et al. 2014), however this risk can be mitigated with disease screening.

The current rate of King Island scrubtit population decline, and the extent to which this decline is exacerbated by genetic effects are currently unknown. Our results suggest two precautionary approaches to genetic management of King Island scrubtits are feasible. Assuming that delaying management will not compromise the chances of future King Island scrubtit population recovery, the Tasman Peninsula subpopulation of Tasmanian scrubtits could be used as a trial for genetic rescue, given the remarkable similarity of this subpopulation's genetic parameters to the King Island scrubtit. If conservation actions are considered urgent, genetic rescue trials could occur in the Pegarah Forest King Island scrubtit subpopulation, which our data suggest is most at risk of inbreeding and extinction, with minimal risks of negative genetic effects spreading to the other two subpopulations via natural gene flow.

Research implications

Field research to understand current vital rates and dispersal dynamics is urgently required to quantify the fitness costs of high inbreeding and low genetic diversity in the King Island scrubtit as these costs can be high (Harrisson et al. 2019; Kardos et al. 2023). The relative contribution of genetic effects associated with the taxon's small and fragmented population to its decline can then be compared to other known threats such as predation by feral cats. This information can help prioritise implementation of recovery actions to address the most prominent threats facing the taxon. We consider two particular priorities are to determine: (1) whether contemporary breeding success and juvenile recruitment in King Island scrubtit are low, and if so whether this is primarily due to inbreeding depression (e.g. Duntsch et al. 2023), high predation rates (e.g. Crates et al. 2019) or simply a severe shortage of breeding resources (i.e. habitat saturation, Komdeur, 1992); and (2) whether any surviving juveniles are able to successfully disperse between subpopulations. Our data suggest successful juvenile dispersal is unlikely, in which case juveniles (i) remain in their natal areas without breeding; (ii) breed with close relatives; or (iii) die during dispersal. Under such scenarios, translocation of juveniles between subpopulations could facilitate genetic rescue with minimal risk to the current effective population (Frankham et al. 2015).

More broadly, our study highlights the potential for avoidable biodiversity loss to occur when the conservation requirements of less enigmatic or geographically remote taxa are overlooked (Woinarski et al. 2017). It also highlights the challenges of implementing effective conservation measures when basic population monitoring data are lacking (Lindenmayer et al. 2020). The conservation status of the King Island scrubtit has been known for decades (Garnett et al. 2011), however targeted research to establish the species' basic ecological requirements is ongoing (Webb et al. 2016, Bell et al. 2023). Population genomics is itself an important tool for implementing evidence-based conservation, but is most effective at preventing extinctions when complemented with rigorous, field-based population monitoring data (Taylor et al. 2017, Duntsch et al.

2023).

ACKNOWLEDGEMENTS

We acknowledge the traditional custodians of the land on which this research was conducted. This study was funded by the Commonwealth Department of Environment and Climate Change, BirdLife Australia and generous donors to the Difficult Bird Research Group. Sequencing received in-kind support from the NCRIS funded BioPlatforms Threatened Species Initiative. Research was conducted under Tasmanian Scientific licence #TFA23010, ANU animal ethics permit #A2021/33 and ABBBS banding authorities #3192 & #2833. Computational resources were provided by Amazon Web Services and RONIN; the Australian Biocommons supported FGENESH++ service; the Pawsey Supercomputing Research Centre with funding from the Australian Government and the Government of Western Australia; Galaxy Australia, a service provided by the Australian Biocommons and its partners; and the University of Sydney's High Performance Computing facility Artemis. We thank Mark Carey, the King Island Conservation Action Plan working group, Sustainable Timber Tasmania, the Tasmanian National Parks and Wildlife Service & H. Camm & family for logistical support. KAF is supported by the Australian Research Council Centre of Excellence for Innovations in Peptide and Protein Science (CE200100012).

AUTHOR CONTRIBUTIONS

RC: Research design, data collection, data analysis, writing- original draft, writing- revisions.

BvT: Data analysis, writing- original draft, writing- revisions.

CY: Data collection, writing- original draft.

DS: Data collection, writing- original draft.

LN: Laboratory assistance, data analysis, writing-original draft.

LM: Data collection.

DG: DNA extraction, writing-original draft.

CH: Data analysis, writing-original draft.

PB: Data collection, writing- original draft.

RH: Writing-original draft.

KF: Data analysis, writing- original draft, writing- revisions.

REFERENCES

Allendorf, F. W., Hohenlohe, P. A., & Luikart, G. (2010). Genomics and the future of conservation genetics. Nature reviews genetics, 11(10), 697-709.

Alves, F., Banks, S., Edworthy, M., Stojanovic, D., Langmore, N. & Heinsohn, R. (2023). Using Conservation genetics to prioritise management options for an endangered songbird. Heredity *In press.*

Barnett, D. W., Garrison, E. K., Quinlan, A. R., Strömberg, M. P., & Marth, G. T. (2011). BamTools: a C++ API and toolkit for analyzing and managing BAM files. Bioinformatics, 27(12), 1691-1692. https://doi.org/10.1093/bioinformatics/btr174.

Bates, D., Mächler, M., Bolker, B., & Walker, S. (2015). Fitting Linear Mixed-Effects Models Using lme4. Journal of Statistical Software, 67(1), 1–48. https://doi.org/10.18637/jss.v067.i01.

Bell, D. A., Robinson, Z. L., Funk, W. C., Fitzpatrick, S. W., Allendorf, F. W., Tallmon, D. A., & Whiteley, A. R. (2019). The exciting potential and remaining uncertainties of genetic rescue. Trends in Ecology & Evolution, 34(12), 1070-1079.

Bell, P. J., Webb, M. H., Holdsworth, M., & Baker, G. B. (2023). Defining and mapping habitat requirements to support the survival of King Island threatened birds. Report to Cradle Coast NRM, Cradle Coast Authority, Burnie, Tasmania.

Benjamini, Y., & Hochberg, Y. (1995). Controlling the false discovery rate: A practical and powerful approach to multiple testing. Journal of the Royal Statistical Society: Series B: Methodological, 57(1), 289– 300.

BirdLife International (2022) Species factsheet: Acanthornis magna. Downloaded from http://www.birdlife.org on 27/10/2022.

Bowdler, S. (2015). The bass strait Islands revisited. Quaternary International, 385, 206-218.

Canessa, S., Taylor, G., Clarke, R. H., Ingwersen, D., Vandersteen, J., & Ewen, J. G. (2020). Risk aversion and uncertainty create a conundrum for planning recovery of a critically endangered species. Conservation Science and Practice, 2(2), e138.

Catchen, J., Hohenlohe, P. A., Bassham, S., Amores, A., & Cresko, W. A. (2013). Stacks: An analysis tool set for population genomics. Molecular Ecology, 22(11), 3124– 3140.

Caye, K., Deist, T., Martins, H., Michel, O., & Francois, O. (2016) TESS3: fast inference of spatial population structure and genome scans for selection. Molecular Ecology Resources 16 (2), 540-548. doi: 10.1111/1755-0998.12471.

Caye, K., Jay, F., Michel, O., & François, O. (2018). Fast inference of individual admixture coefficients using geographic data. Annals of Applied Statistics, 12(1), 586– 608. https://doi.org/10.1214/17-AOAS1106.

Caye, K., Jumentier, B., Lepeule, J., & François, O. (2019). LFMM 2: fast and accurate inference of gene-environment associations in genome-wide studies. Molecular biology and evolution, 36(4), 852-860.

Cheng, D., Yan, X., Qiu, G., Zhang, J, Wang, H., Feng, T., Tian, Y., Xu, H., Wang, M., He, W., Wu, P., Widelitz, R.B., Chuong, C-M., Yue, Z. (2018). Contraction of basal filopodia controls periodic feather branching via Notch and FGF signaling. Nature Communications. 9(1345). Doi:10.1038/s41467-018-03801-z

Cheng, H., Concepcion, G. T., Feng, X., Zhang, H., & Li, H. (2021). Haplotype-resolved de novo assembly using phased assembly graphs with hifiasm. Nature Methods, 18(2), 170-175. https://doi.org/10.1038/s41592-020-01056-5

Cheng, H., Jarvis, E. D., Fedrigo, O., Koepfli, K.-P., Urban, L., Gemmell, N. J., & Li, H. (2022). Haplotype-resolved assembly of diploid genomes without parental data. Nature Biotechnology, 40(9), 1332-1335. https://doi.org/10.1038/s41587-022-01261-x

Commonwealth of Australia (2022). Threatened species action plan 2022-32. Available at https://www.dcceew.gov.au/sites/default/files/documents/threatened-species-action-plan-2022-2032.pdf.

Corney, S., Grose, M., Bennett, J. C., White, C., Katzfey, J., McGregor, J., ... & Bindoff, N. L. (2013). Performance of downscaled regional climate simulations using a variable-resolution regional climate model: Tasmania as a test case. Journal of Geophysical Research: Atmospheres, 118(21), 11-936.

Crates, R., Rayner, L., Stojanovic, D., Webb, M., Terauds, A., & Heinsohn, R. (2019). Contemporary breeding biology of critically endangered regent honeyeaters: implications for conservation. Ibis, 161(3), 521-532.

Danecek, P., Bonfield, J. K., Liddle, J., Marshall, J., Ohan, V., Pollard, M. O., Whitwham, A., Keane, T., McCarthy, S. A., Davies, R. M., & Li, H. (2021). Twelve years of SAMtools and BCFtools. GigaScience, 10(2). https://doi.org/10.1093/gigascience/giab008

DeRaad, D.A. (2022), SNPfiltR: an R package for interactive and reproducible SNP filtering. Molecular Ecology Resources, 00, 1-15. http://doi.org/10.1111/1755-0998.13618.

Do, C., Waples, R. S., Peel, D., Macbeth, G. M., Tillett, B. J., & Ovenden, J. R. (2014). NeEstimator v2: re-implementation of software for the estimation of contemporary effective population size (Ne) from genetic data. Molecular ecology resources, 14(1), 209-214.

Duntsch, L., Whibley, A., de Villemereuil, P., Brekke, P., Bailey, S., Ewen, J. G., & Santure, A. W. Genomic signatures of inbreeding depression for a threatened Aotearoa New Zealand passerine. Molecular Ecology. Doi: 10.1111/mec.16855.

Dyer, R. (2021). gstudio: Tools Related to the Spatial Analysis of Genetic Marker Data. https://github.com/dyerlab/gstudio.

Farquharson, K.A., McLennan, E.A., Cheng, Y., Alexander, L., Fox, S., Lee, A.V., Belov, K. and Hogg, C.J., (2022). Restoring faith in conservation action: Maintaining wild genetic diversity through the Tasmanian devil insurance program. Iscience, 25(7), p.104474.

Frankham, R. (1995). Conservation genetics. Annual review of genetics, 29(1), 305-327.

Frankham, R. (2015). Genetic rescue of small inbred populations: Meta-analysis reveals large and consistent benefits of gene flow. Molecular ecology, 24(11), 2610-2618.

Frankham, R., Ballou, J.D., Ralls, K., Eldridge, M., Dudash, M.R., Fenster, C.B., Lacy, R.C. and Sunnucks, P., 2017. Genetic management of fragmented animal and plant populations. Oxford University Press.

Frichot, E., & Francois, O. (2015). LEA: An R package for landscape and ecological association studies. Methods in Ecology and Evolution, 6(8), 925-929.

Garnett, S. T., Szabo, J. K., and Dutson, G. (2011). Action Plan for Australian Birds 2010. CSIRO Publishing, Melbourne.

Geyle, H. M., Woinarski, J.C.Z., Baker, G.B., Dickman, C.R., Dutson, G., Fisher, D.O., Ford, H. et al. "Quantifying extinction risk and forecasting the number of impending Australian bird and mammal extinctions." Pacific Conservation Biology 24, no. 2 (2018): 157-167.

Hogg, J. T., Forbes, S. H., Steele, B. M., & Luikart, G. (2006). Genetic rescue of an insular population of large mammals. Proceedings of the Royal Society B: Biological Sciences, 273(1593), 1491-1499.

Hogg, C.J., Wright, B., Morris, K.M., Lee, A.V., Ivy, J.A., Grueber, C.E. and Belov, K., 2019. Founder relationships and conservation management: empirical kinships reveal the effect on breeding programmes when founders are assumed to be unrelated. Animal Conservation, 22(4), pp.348-361.

Fielding, M. W., Cunningham, C. X., Buettel, J. C., Stojanovic, D., Yates, L. A., Jones, M. E., & Brook, B. W. (2022). Dominant carnivore loss benefits native avian and invasive mammalian scavengers. Proceedings of the Royal Society B, 289(1985), 20220521.

Frankham, R. (1995). Conservation genetics. Annual review of genetics, 29(1), 305-327.

Frankham R, Bradshaw CJA, Brook BW (2014) Genetics in conservation management: revised recommendations for the 50/500 rules, Red List criteria and population viability analyses. Biological Conservation, 170, 56–63.

Frankham, R., Bradshaw, C., & Brook, B. (2014). 50/500 rules need upward revision to 100/1000:–Response to Franklin et al. Biological Conservation, 176, 286-286.

Frankham, R. (2015). Genetic rescue of small inbred populations: meta-analysis reveals large and consistent benefits of gene flow. Molecular Ecology 24, 2610-2618.

Frichot, E., & Francois, O. (2015). LEA: An R package for landscape and ecological association studies. Methods in Ecology and Evolution, 6(8), 925– 929. https://doi.org/10.1111/2041-210X.12382.

Frichot, E., Mathieu, F., Trouillon, T., Bouchard, G., & Francois, O. (2014). Fast and efficient estimation of individual ancestry coefficients. Genetics, 196(4), 973– 983. https://doi.org/10.1534/genetics.113.160572.

Fridolfsson A-K, and Ellegren H (1999) A simple and universal method for molecular sexing of non-ratite birds. Journal of Avian Biology 30:116-121.

Gruber, B., & Adamack, A. (2022). PopGenReport: A Simple Framework to Analyse Population and Landscape Genetic Data. https://cran.r-project.org/web/packages/PopGenReport/index.html.

Harrisson, K. A., Pavlova, A., Goncalves da Silva, A., Rose, R., Bull, J. K., Lancaster, M. L., ... & Sunnucks, P. (2016). Scope for genetic rescue of an endangered subspecies though re-establishing natural gene flow with another subspecies. Molecular Ecology, 25(6), 1242-1258.

Higgins, P., Peter, J., & Cowling, S. (eds). (2006). Handbook of Australian, New Zealand & Antarctic birds Volume 7: Boatbills to Starlings. Oxford University Press, Melbourne, Australia.

Johnson, M., Zaretskaya, I., Raytselis, Y., Merezhuk, Y., McGinnis, S., Madden, T.L. (2008). NCBI BLAST: a better web interface. Nucleic Acids Research. 36(2):W5-W9. doi:10.1093/nar/gkn201.

Jones, M. E., Paetkau, D., Geffen, E. L. I., & Moritz, C. (2004). Genetic diversity and population structure of Tasmanian devils, the largest marsupial carnivore. Molecular Ecology, 13(8), 2197-2209.

Kardos, M., Zhang, Y., Parsons, K.M. et al. Inbreeding depression explains killer whale population dynamics. Nat Ecol Evol (2023). https://doi.org/10.1038/s41559-023-01995-0.

Kamvar, Z.N. (2023). Package 'poppr'. Genetic analysis of populations with mixed reproductions. https://cran.r-project.org/web/packages/poppr/poppr.pdf.

Keenan, K., McGinnity, P., Cross, T. F., Crozier, W. W., & Prodohl, P. A. (2013). diveRsity: An R package for the estimation and exploration of population genetics parameters and their associated errors. Methods in ecology and evolution, 4(8), 782-788.

Kim, S. Y., Lohmueller, K. E., Albrechtsen, A., Li, Y., Korneliussen, T., Tian, G., Grarup, N., Jiang, T., Andersen, G., Witte, D., Jorgensen, T., Hansen, T., Pedersen, O., Wang, J., & Nielsen, R. (2011). Estimation of allele frequency and association mapping using next-generation sequencing data. BMC Bioinformatics, 12(1), 231. https://doi.org/10.1186/1471-2105-12-231.

Komdeur, J. (1992). Importance of habitat saturation and territory quality for evolution of cooperative breeding in the Seychelles warbler. Nature, 358(6386), 493-495.

Korneliussen, T. S., Albrechtsen, A., & Nielsen, R. (2014). Open access ANGSD: Analysis of next generation sequencing data. BMC Bioinformatics, 15(356), 1– 13.

Lachish, S., Bonsall, M. B., Lawson, B., Cunningham, A. A., & Sheldon, B. C. (2012). Individual and population-level impacts of an emerging poxvirus disease in a wild population of great tits. PLoS One, 7(11), e48545.

Li H. and Durbin R. (2009) Fast and accurate short read alignment with Burrows-Wheeler transform. Bioinformatics, 25, 1754-1760.

Li, H. (2013). Aligning sequence reads, clone sequences and assembly contigs with BWA-MEM. ArXiv:1303.3997 [q-Bio]. http://arxiv.org/abs/1303.3997.

Lindenmayer, D., Woinarski, J., Legge, S., Southwell, D., Lavery, T., Robinson, N., ... & Wintle, B. (2020). A checklist of attributes for effective monitoring of threatened species and threatened ecosystems. Journal of environmental management, 262, 110312.

Lynch, M. (1991). The genetic interpretation of inbreeding depression and outbreeding depression. Evolution, 45(3), 622-629.

Manni M., Berkeley, M.R., Seppey, M., Simao, F.A., Zdobnov, E.M. BUSCO Update: Novel and Streamlined Workflows along with Broader and Deeper Phylogenetic Coverage for Scoring of Eukaryotic, Prokaryotic, and Viral Genomes, Molecular Biology and Evolution, Volume 38, Issue 10, October 2021, Pages 4647–4654, https://doi.org/10.1093/molbev/msab199

Martins, H., Caye, K., Luu, K., Blum, M. G., & Francois, O. (2016). Identifying outlier loci in admixed and in continuous populations using ancestral population differentiation statistics. Molecular ecology, 25(20), 5029-5042.

Moritz, C. (1994). Defining 'evolutionarily significant units' for conservation. Trends in ecology & evolution, 9(10), 373-375.

O'Leary, S. J., Puritz, J. B., Willis, S. C., Hollenbeck, C. M., & Portnoy, D. S. (2018). These aren't the loci you'e looking for: Principles of effective SNP filtering for molecular ecologists. Molecular Ecology, 27(16), 3193– 3206. https://doi.org/10.1111/mec.14792.

Pavlova, A., Selwood, P., Harrisson, K. A., Murray, N., Quin, B., Menkhorst, P., ... & Sunnucks, P. (2014). Integrating phylogeography and morphometrics to assess conservation merits and inform conservation strategies for an endangered subspecies of a common bird species. Biological Conservation, 174, 136-146.

Pembleton, L. W., Cogan, N. O., & Forster, J. W. (2013). St AMPP: An R package for calculation of genetic differentiation and structure of mixed-ploidy level populations. Molecular ecology resources, 13(5), 946-952.

Peters, A., Patterson, E. I., Baker, B. G., Holdsworth, M., Sarker, S., Ghorashi, S. A., & Raidal, S. R. (2014). Evidence of psittacine beak and feather disease virus spillover into wild critically endangered orange-bellied parrots (Neophema chrysogaster). Journal of Wildlife Diseases, 50(2), 288-296.

Peterson, B. K., Weber, J. N., Kay, E. H., Fisher, H. S., & Hoekstra, H. E. (2012). Double digest RADseq: an inexpensive method for de novo SNP discovery and genotyping in model and non-model species. PloS one, 7(5), e37135.

Price, G., & Farquharson, K. (2022). PacBio HiFi genome assembly using hifiasm v2.1. WorkflowHub. https://doi.org/10.48546/WORKFLOWHUB.WORKFLOW.221.3

R Core Team. (2020). R: A language and environment for statistical computing. R Foundation for Statistical Computing. http://www.r-project.org.

Ralls, K., Ballou, J.D., Dudash, M.R., Eldridge, M.D., Fenster, C.B., Lacy, R.C., Sunnucks, P. and Frankham, R., 2018. Call for a paradigm shift in the genetic management of fragmented populations. Conservation Letters, 11(2), p.e12412.

Robledo-Ruiz, D., Gan, H. M., Kaur, P., Dudchenko, O., Weisz, D., Khan, R., Aiden, E. L., Osipova, E., Hiller, M., Morales, H. E., Magrath, M. J., Clarke, R. H., Sunnucks, P. & Pavlova, A. (2022) Chromosome-length genome assembly and linkage map of a critically endangered Australian bird: the helmeted honeyeater, GigaScience 11, giac025, https://doi.org/10.1093/gigascience/giac025.

Robledo-Ruiz, D., Austin, L., Amos, J., Castrejon-Figureoa, J., Harley, D., Magrath, M., Sunnucks, P. & Pavlova, A. (In Press). Easy-to-use R functions to separate reduced-representation genomic datasets into sex-linked and autosomal loci, and conduct sex-assignment. Molecular Ecology Resources.

Roelke, M. E., Martenson, J. S., & O'Brien, S. J. (1993). The consequences of demographic reduction and genetic depletion in the endangered Florida panther. Current Biology, 3(6), 340-350.

Rousset F. (1997). Genetic differentiation and estimation of gene flow from F-statistics under isolation by distance. Genetics 145: 1219–1228. pmid:9093870.

Solovyev, V., Kosarev, P., Seledsov, I., & Vorobyev, D. (2006). Automatic annotation of eukaryotic genes, pseudogenes and promoters. Genome Biology, 7(1), S10. https://doi.org/10.1186/gb-2006-7-s1-s10

Stoffel, M. A., Esser, M., Kardos, M., Humble, E., Nichols, H., David, P., & Hoffman, J. I. (2016). inbreedR: an R package for the analysis of inbreeding based on genetic markers. Methods in Ecology and Evolution, 7(11), 1331-1339.

Stojanovic, D., Neeman, T., Lacy, R., Farquharson, K. A., Hogg, C. J., & Heinsohn, R. (2022). Effects of non-random juvenile mortality on small, inbred populations. Biological Conservation, 268, 109504.

Sutherland, W. J., Pullin, A. S., Dolman, P. M., & Knight, T. M. (2004). The need for evidence-based conservation. Trends in ecology & evolution, 19(6), 305-308.

Tallmon, D. A., Luikart, G., & Waples, R. S. (2004). The alluring simplicity and complex reality of genetic rescue. Trends in Ecology & Evolution, 19(9), 489-496.

Taylor H. R, Dussex, N., van Heezik, Y. (2017). Bridging the conservation genetics gap by identifying barriers to implementation for conservation practitioners. Global Ecology & Conservation 10: 231–242.

The Galaxy Community. (2022). The Galaxy platform for accessible, reproducible and collaborative biomedical analyses: 2022 update. Nucleic Acids Research, 50(W1), W345-W351. https://doi.org/10.1093/nar/gkac247

Threatened Species Section (2012). King Island Biodiversity Management Plan. Department of Primary Industries, Parks, Water and Environment, Hobart.

Thys, B., Pinxten, R., Raap, T., De Meester, G., Rivera-Gutierrez, H. F., & Eens, M. (2017). The female perspective of personality in a wild songbird: repeatable aggressiveness relates to exploration behaviour. Scientific Reports, 7(1), 7656.

Uliano-Silva, M., Ferreira, J.G.R.N., Krasheninnikova, K. et al. MitoHiFi: a python pipeline for mitochondrial genome assembly from PacBio high fidelity reads. BMC Bioinformatics 24, 288 (2023). https://doi.org/10.1186/s12859-023-05385-y

van Velden, J. L., Koeslag, A., Curtis, O., Gous, T., & Amar, A. (2017). Negative effect of mite (Knemidokoptes) infection on reproductive output in an African raptor. The Auk: Ornithological Advances, 134(3), 498-508.

von Takach, B., Ahrens, C. W., Lindenmayer, D. B., & Banks, S. C. (2021). Scale-dependent signatures of local adaptation in a foundation tree species. Molecular Ecology, 30(10), 2248-2261.

von Takach, B., Ranjard, L., Burridge, C. P., Cameron, S. F., Cremona, T., Eldridge, M. D., ... & Banks, S. C. (2022). Population genomics of a predatory mammal reveals patterns of decline and impacts of exposure to toxic toads. Molecular Ecology, 31(21), 5468-5486.

von Takach, B., Sargent, H., Penton, C. E., Rick, K., Murphy, B. P., Neave, G., ... & Banks, S. C. (2023). Population genomics and conservation management of the threatened black-footed tree-rat (Mesembriomys gouldii) in northern Australia. Heredity, 1-11.

Wang, J., 2007. Triadic IBD coefficients and applications to estimating pairwise relatedness. Genetics Research, 89(3), pp.135-153.

Wang, J. (2011). COANCESTRY: a program for simulating, estimating and analysing relatedness and inbreeding coefficients. Molecular ecology resources, 11(1), 141-145.

Waples, R. S. (2015). Testing for Hardy–Weinberg proportions: have we lost the plot?. Journal of heredity, 106(1), 1-19.

Webb, M. H., Holdsworth, M., Stojanovic, D., Terauds, A., Bell, P., & Heinsohn, R. (2016). Immediate action required to prevent another Australian avian extinction: the King Island Scrubtit. Emu-Austral Ornithology, 116(3), 223-229.

Webb, M.H., Stojanovic, D. & Heinsohn, R. (2018). Policy failure and conservation paralysis for the critically endangered swift parrot. Pacific Conserv. Biol. 25, 116–123.

Weeks, A. R., Heinze, D., Perrin, L., Stoklosa, J., Hoffmann, A. A., van Rooyen, A., ... & Mansergh, I. (2017). Genetic rescue increases fitness and aids rapid recovery of an endangered marsupial population. Nature Communications, 8(1), 1071.

Weir, B. S., & Cockerham, C. C. (1984). Estimating F-statistics for the analysis of population structure. Evolution, 38(6), 1358– 1370. https://doi.org/10.1111/j.1558-5646.1984.tb05657.x

Whitlock, M.C. and Lotterhos K.J. (2015) Reliable detection of loci responsible for local adaptation: inference of a neutral model through trimming the distribution of Fst. The American Naturalist 186: 24 - 36.

Willi, Y., Kristensen, T. N., Sgro, C. M., Weeks, A. R., Orsted, M., & Hoffmann, A. A. (2022). Conservation genetics as a management tool: The five best-supported paradigms to assist the management of threatened species. Proceedings of the National Academy of Sciences, 119(1), e2105076119.

Woinarski, J. C., Garnett, S. T., Legge, S. M., & Lindenmayer, D. B. (2017). The contribution of policy, law, management, research, and advocacy failings to the recent extinctions of three Australian vertebrate species. Conservation Biology, 31(1), 13-23.

Yang J, Benyamin B, McEvoy BP, Gordon S, Henders AK, Nyholt DR, Madden PA, Heath AC, Martin NG, Montgomery GW, Goddard ME, Visscher PM. 2010. Common SNPs explain a large proportion of the heritability for human height. Nat Genet. 42(7):565-9. Epub 2010 Jun 20.

Zheng, X., Levine, D., Shen, J., Gogarten, S. M., Laurie, C., & Weir, B. S. (2012). A high-performance computing toolset for relatedness and principal component analysis of SNP data. Bioinformatics, 28(24), 3326– 3328. https://doi.org/10.1093/bioinformatics/bts606.

DATA ACCESSIBILITY AND BENEFIT-SHARING

Related metadata and code, including georeferences in decimal degrees and date/month/year of sampling event and unique sample identifier tags that can be matched to the deposited genetic data, is available in the online supplementary material and via the Dryad digital repository https://doi.org/10.5061/dryad.wstqjq2ss. The genome assembly and raw transcriptome data will be made available under NCBI's BioProject PRJNA1014961. The raw PacBio HiFi reads are publicly available from the Bioplatforms Australia Threatened Species Initiative: https://data.bioplatforms.com/organization/threatened-species. The assembled genome, global transcriptome, and genome annotation generated in this study are available on Amazon Web Services Australasian Genomes Open Data Store: https://awgg-lab.github.io/australasiangenomes/genomes.html.

Benefits Generated: A research collaboration was developed between three academic institutions, a non-governmental organisation, state and federal governments and the local community on King Island. Results of the research will be used to directly inform conservation actions to help facilitate population recovery of the King Island scrubtit and will be used indirectly to help inform genetic management of other small, isolated animal populations both within Australia and globally. Additional benefits from this research accrue from the sharing of our data and results on public databases as described above.

SUPPLEMENTARY INFORMATION

Supplementary file S1: Additional information on methods

Molecular sexing

We determined the sex of individuals using a polymerase chain reaction (PCR) protocol adapted from Fridolfsson and Ellegren (1999). We used 0.25µL forward primer *2550F,* 0.25µL reverse primer *2718R*and 6.25µL One*Taq*® DNA Polymerase (*New England BioLabs* , Victoria, Australia) in combination with 1µL DNA for each of the 12.5µL reactions. We used an *Eppendorf*® *Mastercycler* machine with an annealing

temperature of 48°C. To visualise the reactions, we ran the PCRs at 100V for 30 minutes on a 1.5% agarose gel with *sybr*stain (*Invitrogen* , NSW, Australia). Males were identified through the amplification of a single product while two products were visible for females.

Library preparation

The library preparation protocol consisted of (i) digestion using the aforementioned restriction enzymes (ii) ligation with one of 48 unique inline barcoded adapters compatible with the restriction site overhang, (iii) manual sample pooling, (iv) DNA purification (QIAquick PCR Purification Kit followed by SPRIselect paramagnetic beads), (v) 62 bp narrow size-selection targeting fragments of 280– 342 bp in length (BluePippin, Sage Science) and (vi) a PCR (polymerase chain reaction) amplification step where one of two multiplexing index primers was added. Indexed libraries were pooled together and loaded onto flow cells for 150- bp paired-end sequencing on an Illumina NovaSeq 6000 platform.

Bioinformatics pipeline

Raw sequence data were demultiplexed using the *process_radtags*function of Stacks (Catchen et al., 2013), with checking for intact RAD sites and reads quality-checked and trimmed. Of the 503.8 million total reads, 99.9% were retained after demultiplexing. Trimmomatic v0.39 (Bolger et al., 2014) was used to remove possible adapter contamination, and reads were aligned to the reference genome assembled in this study with BWA v0.7.17-r1188 (Li & Durbin, 2009). All samples mapped well (mean mapping rate = 95.16%; SD = 0.67, range = 92.83–96.46%). The*gstacks* function of Stacks was used to call a catalogue of variants, filtered with the *populations* function by retaining variants in with a minor allele frequency of 0.01; maximum heterozygosity of 0.8; genotyped in 30% of samples; and retaining only one SNP per tag (–write-random-snp). SNPs were filtered using a custom R script to retain SNPs with a minimum average allelic depth of 2.5× per allele; a coverage difference between alleles of [?] 80%; a genotyping rate per locus [?] 80%; and a reproducibility of genotype calls between replicates of 100% (Wright et al., 2019). The mean error rate between replicate pairs was 1.17% (SD = 5.58; range = 0.60–2.19%). Further filtering of the SNPs is outlined in Table S2.

Effective population size estimation

We used NeEstimator v.2 (Do et al. 2014) via the "dartR" wrapper to try to estimate the current effective sizes of the King Island and Tasmanian scrubtit populations, using the linkage disequilibrium method with no singleton alleles. We also estimated the effective size of (i) each a-priori scrubtit subpopulation based on sampling locations; and (ii) the 'east coast' and 'rest of the mainland' Tasmanian scrubtit populations. We used this approach based on the results of the population structure analysis and given the NeEstimator algorithm assumes random mating and non-overlapping generations (Do et al. 2014) which are both unlikely to be the case for scrubtits (see results).

Supplementary file S2: Genome sequencing and assembly methodology

Sample collection and DNA/RNA extraction

A single adult male Tasmanian scrubtit was captured using a mist net at Weilangta Forest in south-eastern Tasmania and transported immediately to Hobart where it was euthanized by a veterinary surgeon (Australian National University Animal Research Authority A2021/33). The sample was dissected at the Tasmanian Museum and Art Gallery specimens collection, where brain and organ tissue were preserved in RNALater before being stored at -80@C. High molecular weight (HMW) DNA was extracted from heart and kidney tissue using the Nanobind Tissue Big DNA Kit v1.0 11/19 (Circulomics). A Qubit fluorometer was used to assess the concentration of DNA with the Qubit dsDNA BR assay kit (Thermo Fisher Scientific). RNA was extracted from six organs preserved in RNALater, using the RNeasy Plus Mini Kit (Qiagen) with RNAse-free DNAse (Qiagen) digestion. Extractions were performed using tissue from the heart, brain, spleen, kidney, liver and gonads.

Library construction and sequencing

HMW DNA was sent for PacBio HiFi library preparation with Pippin Prep and sequencing on one single molecule real-time (SMRT) cell of the PacBio Sequel II (Australian Genome Research Facility, Brisbane, Australia).

Total RNA was sequenced as 100 bp paired-end reads using Illumina NovaSeq 6000 with Illumina Stranded mRNA library preparation at the Ramaciotti Centre for Genomics (University of New South Wales, Sydney, Australia).

Genome assembly

Genome assembly was conducted on Galaxy Australia (The Galaxy Community, 2022) following the genome assembly guide (Price & Farquharson, 2022). HiFiAdapterFilt was used to remove adapter sequence in the raw PacBio HiFi reads (Sim et al., 2022), followed by assembly with HiFiasm v0.16.1 with default parameters (Cheng et al., 2021; Cheng et al., 2022).

The quality of the genome assembly was assessed on Galaxy Australia with the genome assessment post-assembly workflow (Price, 2023). Basic genome assembly statistics were calculated with QUAST v5.0.2 (Mikheenko et al., 2018). Completeness was assessed using Benchmarking Universal Single-Copy Orthologs (BUSCO) v5.2.2 (Simão et al., 2015) with the Aves_odb10 lineage (n = 8,338 BUSCOs). The repetitive elements of the genome were identified and classified by building a custom database using RepeatModeler v2.0.1 (Flynn et al., 2020) and RepeatMasker v4.0.9 (Smit et al., 2013-2015) with the -nolow parameter to avoid masking of simple low-complexity repeats, run on a Pawsey Supercomputing Centre Nimbus cloud machine (256 GB RAM, 64 vCPU, 3 TB storage).

Mitogenome assembly

The mitochondrial genome was assembled from the primary genome assembly using MitoHiFi v3 (Uliano-Silva et al., 2022). MitoHiFi identified the rock warbler *Origma solitaria* (NCBI reference sequence NC_053100.1; Feng et al., 2020) as the most closely-related publicly available mitochondrial genome. The mitochondrial genome was visualised with MitoZ v2.3 (Meng et al., 2019).

Transcriptome assembly

Transcriptome assembly was conducted on the University of Sydney High Performance Computer, Artemis. FastQC v0.11.8 (Andrews, 2010) was used to assess the quality of raw reads. Trimmomatic v0.39 (Bolger et al., 2014) was used to quality trim reads specifying TruSeq3-PE adapters, SLIDINGWINDOW:4:5, LEADING:5, TRAILING:5 and MINLEN:25. The repeat-masked genome was indexed and reads aligned with HiSat2 v2.1.0 (Kim et al., 2019). SamTools v1.9 view and sort converted the files to coordinate-sorted BAM format. A GTF for each transcriptome was generated with StringTie v2.1.6 (Pertea et al., 2015). Aligned RNAseq reads were merged into transcripts and filtered to remove transcripts found in only one tissue with fragments per kilobase of transcript per million mapped fragments (FPKM) < 0.1, using TAMA-merge v2020/12/17 (Kuo et al., 2020) and CPC2 v2019-11-19 (Kang et al., 2017). TransDecoder v2.0.1 (Haas, 2022) predicted open reading frames in the resulting global transcriptome. The completeness of the global transcriptome was assessed using BUSCO v5.2.2 in 'transcriptome' mode with the Aves_odb10 lineage on Galaxy Australia.

Genome annotation

Genome annotation was performed using FGENESH++ v7.2.2 (Softberry; (Solovyev et al., 2006)) on a Pawsey Supercomputing Centre Nimbus cloud machine (256 GB RAM, 64 vCPU, 3 TB storage) using the longest open reading frame predicted from the global transcriptome, non-mammalian settings, and optimised parameters supplied with the *Corvus brachyrhynchos* (American crow) gene-finding matrix. BUSCO v5.2.2 in 'protein' mode was used to assess the completeness of the annotation with the Aves_odb10 lineage on Galaxy Australia.

Supplementary References*

Allio, R., Schomaker-Bastos, A., Romiguier, J., Prosdocimi, F., Nabholz, B., & Delsuc, F. (2020). MitoFinder: Efficient automated large-scale extraction of mitogenomic data in target enrichment phylogenomics.*Molecular Ecology Resources* , *20* (4), 892-905. https://doi.org/https://doi.org/10.1111/1755-0998.13160

Andrews, S. (2010). *FastQC: A quality control tool for high throughput sequence data* . http://www.bioinformatics.babraham.ac.uk/projects/fastqc/

Barnett, D. W., Garrison, E. K., Quinlan, A. R., Stromberg, M. P., & Marth, G. T. (2011). BamTools: a C++ API and toolkit for analyzing and managing BAM files. *Bioinformatics* , *27* (12), 1691-1692. https://doi.org/10.1093/bioinformatics/btr174.

Bell, P. J., Webb, M. H., Holdsworth, M., & Baker, G. B. (2023). Defining and mapping habitat. requirements to support the survival of King Island threatened birds. Report to Cradle Coast NRM, Cradle Coast Authority, Burnie, Tasmania.

Bolger, A. M., Lohse, M., & Usadel, B. (2014). Trimmomatic: a flexible trimmer for Illumina sequence data. *Bioinformatics* ,*30* (15), 2114-2120. https://doi.org/10.1093/bioinformatics/btu170

Bushnell, B. (2022). *BBMap* . Retrieved February 2022 from sourceforge.net/projects/bbmap/

Cheng, H., Concepcion, G. T., Feng, X., Zhang, H., & Li, H. (2021). Haplotype-resolved de novo assembly using phased assembly graphs with hifiasm. *Nature Methods* , *18* (2), 170-175. https://doi.org/10.1038/s41592-020-01056-5

Cheng, H., Jarvis, E. D., Fedrigo, O., Koepfli, K.-P., Urban, L., Gemmell, N. J., & Li, H. (2022). Haplotype-resolved assembly of diploid genomes without parental data. *Nature Biotechnology* ,*40* (9), 1332-1335. https://doi.org/10.1038/s41587-022-01261-x

Danecek, P., Bonfield, J. K., Liddle, J., Marshall, J., Ohan, V., Pollard, M. O., Whitwham, A., Keane, T., McCarthy, S. A., Davies, R. M., & Li, H. (2021). Twelve years of SAMtools and BCFtools.*GigaScience* , *10* (2). https://doi.org/10.1093/gigascience/giab008

Do, C., Waples, R. S., Peel, D., Macbeth, G. M., Tillett, B. J., & Ovenden, J. R. (2014). NeEstimator v2: re-implementation of software for the estimation of contemporary effective population size (Ne) from genetic data. Molecular ecology resources, 14(1), 209-214.

Eiler, A., Lofgren, A., Hjerne, O., Norden, S., & Saetra, P. (2018). Environmental DNA (eDNA) detects the pool frog (*Pelophylax lessonae*) at times when traditional monitoring methods are insensitive.*SCIENTIFIC REPORTS* , *8* , 5452. https://doi.org/10.1038/s41598-018-23740-5

Feng, S., Stiller, J., Deng, Y. *et al.* Dense sampling of bird diversity increases power of comparative genomics. *Nature* **587** , 252–257 (2020). https://doi.org/10.1038/s41586-020-2873-9

Flynn, J. M., Hubley, R., Goubert, C., Rosen, J., Clark, A. G., Feschotte, C., & Smit, A. F. (2020). RepeatModeler2 for automated genomic discovery of transposable element families. *Proc Natl Acad Sci U S A* , *117* (17), 9451-9457. https://doi.org/10.1073/pnas.1921046117

Haas, B. J. (2022). *TransDecoder (find coding regions within transcripts)* . Retrieved February 2022 from https://github.com/TransDecoder/TransDecoder

IUCN SSC Amphibian Specialist Group. (2022). *Taudactylus pleione. The IUCN Red List of Threatened Species 2022:e.T21533A78446285.*Retrieved 31st March from https://dx.doi.org/10.2305/IUCN.UK.2022-2.RLTS.T21533A78446285.en

Kang, Y.-J., Yang, D.-C., Kong, L., Hou, M., Meng, Y.-Q., Wei, L., & Gao, G. (2017). CPC2: a fast and accurate coding potential calculator based on sequence intrinsic features. *Nucleic Acids Research* ,*45* (W1), W12-W16. https://doi.org/10.1093/nar/gkx428

Kim, D., Paggi, J. M., Park, C., Bennett, C., & Salzberg, S. L. (2019). Graph-based genome alignment and genotyping with HISAT2 and HISAT-genotype. *Nature Biotechnology* , *37* (8), 907-915. https://doi.org/10.1038/s41587-019-0201-4

Kuo, R. I., Cheng, Y., Zhang, R., Brown, J. W. S., Smith, J., Archibald, A. L., & Burt, D. W. (2020). Illuminating the dark side of the human transcriptome with long read transcript sequencing. *BMC Genomics* ,*21* (1), 751. https://doi.org/10.1186/s12864-020-07123-7

Li H. and Durbin R. (2009) Fast and accurate short read alignment with Burrows-Wheeler transform. *Bioinformatics* , **25** , 1754-1760.

Meng, G., Li, Y., Yang, C., & Liu, S. (2019). MitoZ: a toolkit for animal mitochondrial genome assembly, annotation and visualization.*Nucleic Acids Research* , *47* (11), e63-e63. https://doi.org/10.1093/nar/gkz173

Mikheenko,A., Prjibelski, A., Saveliev, V., Antipov, D., Gurevich, A., Versatile genome assembly evaluation with QUAST-LG, Bioinformatics (2018) 34 (13): i142-i150. doi: 10.1093/bioinformatics/bty266 First published online: June 27, 2018

Pertea, M., Pertea, G. M., Antonescu, C. M., Chang, T. C., Mendell, J. T., & Salzberg, S. L. (2015). StringTie enables improved reconstruction of a transcriptome from RNA-seq reads. *Nat Biotechnol* ,*33* (3), 290-295. https://doi.org/10.1038/nbt.3122

Price, G., & Farquharson, K. (2022). PacBio HiFi genome assembly using hifiasm v2.1. WorkflowHub. https://doi.org/10.48546/WORKFLOWHUB.WORKFLOW.221.3

Price, G. (2023). Genome assessment post assembly. WorkflowHub. https://doi.org/10.48546/WORKFLOWHUB.WORKFLOW.403.2

Simao, F. A., Waterhouse, R. M., Ioannidis, P., Kriventseva, E. V., & Zdobnov, E. M. (2015). BUSCO: assessing genome assembly and annotation completeness with single-copy orthologs. *Bioinformatics* ,*31* (19), 3210-3212. https://doi.org/10.1093/bioinformatics/btv351

Smit, A. F. A., Hubley, R., & Green, P. (2013-2015). *RepeatMasker Open-4.0* . Retrieved February 2022 from http://www.repeatmasker.org

Solovyev, V., Kosarev, P., Seledsov, I., & Vorobyev, D. (2006). Automatic annotation of eukaryotic genes, pseudogenes and promoters.*Genome Biology* , *7* (1), S10. https://doi.org/10.1186/gb-2006-7-s1-s10

Sim, S.B., Corpuz, R.L., Simmonds, T.J. *et al.* HiFiAdapterFilt, a memory efficient read processing pipeline, prevents occurrence of adapter sequence in PacBio HiFi reads and their negative impacts on genome assembly. *BMC Genomics* **23** , 157 (2022). https://doi.org/10.1186/s12864-022-08375-1

Sun, Y. B., Zhang, Y., & Wang, K. (2020). Perspectives on studying molecular adaptations of amphibians in the genomic era. *Zool Res* ,*41* (4), 351-364. https://doi.org/10.24272/j.issn.2095-8137.2020.046

The Galaxy Community. (2022). The Galaxy platform for accessible, reproducible and collaborative biomedical analyses: 2022 update.*Nucleic Acids Research* , *50* (W1), W345-W351. https://doi.org/10.1093/nar/gkac247

Uliano-Silva, M., Gabriel R. N. Ferreira, J., Krasheninnikova, K., Formenti, G., Abueg, L., Torrance, J., Myers, E. W., Durbin, R., Blaxter, M., & McCarthy, S. A. (2023). MitoHiFi: a python pipeline for mitochondrial genome assembly from PacBio High Fidelity reads.*bioRxiv* , 2022.2012.2023.521667. https://doi.org/10.1101/2022.12.23.521667

Vurture, G. W., Sedlazeck, F. J., Nattestad, M., Underwood, C. J., Fang, H., Gurtowski, J., & Schatz, M. C. (2017). GenomeScope: fast reference-free genome profiling from short reads. *Bioinformatics* ,*33* (14), 2202-2204. https://doi.org/10.1093/bioinformatics/btx153

Webb, M. H., Holdsworth, M., Stojanovic, D., Terauds, A., Bell, P., & Heinsohn, R. (2016). Immediate action required to prevent another Australian avian extinction: the King Island Scrubtit. Emu-Austral Ornithology, 116(3), 223-229.

Wright, B., Farquharson, K.A., McLennan, E.A., Belov, K., Hogg, C.J., Grueber, C.E. (2019). From reference genomes to population genomics: comparing three reference-aligned reduced-representation sequencing pipelines in two wildlife species. BMC Genomics. 20(453). doi:10.1186/s12864-019-5806-y

Supplementary Tables

Table S1: King Island and Tasmanian scrubtit sample metadata.

Source	Sample	Specimen	Tissue	Pres.	Taxon	Scientific name	Collecti
population	id	id	type	Temp.	id		date
Weilangta	407004	ANU-ST67	Muscle in EtOh	-80	720576	*Acanthornis magna magna*	14/04/2
Weilangta	407008	ANU-ST67	Muscle in EtOh	-80	720576	*Acanthornis magna magna*	14/04/2
Colliers Swamp	406973	ANU-ST36	Blood in EtOh	-80	720576	*Acanthornis magna greeniana*	7/04/20
Colliers Swamp	406974	ANU-ST37	Blood in EtOh	-80	720576	*Acanthornis magna greeniana*	7/04/20
Colliers Swamp	406975	ANU-ST38	Blood in EtOh	-80	720576	*Acanthornis magna greeniana*	7/04/20
Colliers Swamp	406976	ANU-ST39	Blood in EtOh	-80	720576	*Acanthornis magna greeniana*	7/04/20
Colliers Swamp	406977	ANU-ST40	Blood in EtOh	-80	720576	*Acanthornis magna greeniana*	7/04/20
Nook	406978	ANU-ST41	Blood in EtOh	-80	720576	*Acanthornis magna greeniana*	9/04/20
Nook	406979	ANU-ST42	Blood in EtOh	-80	720576	*Acanthornis magna greeniana*	9/04/20
Nook	406980	ANU-ST43	Blood in EtOh	-80	720576	*Acanthornis magna greeniana*	9/04/20
Nook	406981	ANU-ST44	Blood in EtOh	-80	720576	*Acanthornis magna greeniana*	9/04/20
Nook	406982	ANU-ST45	Blood in EtOh	-80	720576	*Acanthornis magna greeniana*	9/04/20
Nook	407012	ANU-ST43	Blood in EtOh	-80	720576	*Acanthornis magna greeniana*	9/04/20
Pegarah	406983	ANU-ST46	Blood in EtOh	-80	720576	*Acanthornis magna greeniana*	10/04/2
Pegarah	406984	ANU-ST47	Blood in EtOh	-80	720576	*Acanthornis magna greeniana*	10/04/2
Pegarah	406985	ANU-ST48	Blood in EtOh	-80	720576	*Acanthornis magna greeniana*	10/04/2
Pegarah	406986	ANU-ST49	Blood in EtOh	-80	720576	*Acanthornis magna greeniana*	10/04/2
Pegarah	406987	ANU-ST50	Blood in EtOh	-80	720576	*Acanthornis magna greeniana*	10/04/2
Central North	406988	ANU-ST51	Blood in EtOh	-80	720576	*Acanthornis magna magna*	12/04/2
Central North	406989	ANU-ST52	Blood in EtOh	-80	720576	*Acanthornis magna magna*	12/04/2
Central North	406990	ANU-ST53	Blood in EtOh	-80	720576	*Acanthornis magna magna*	12/04/2
Central North	406991	ANU-ST54	Blood in EtOh	-80	720576	*Acanthornis magna magna*	12/04/2
Central North	406992	ANU-ST55	Blood in EtOh	-80	720576	*Acanthornis magna magna*	12/04/2
Central North	406993	ANU-ST56	Blood in EtOh	-80	720576	*Acanthornis magna magna*	12/04/2
Central North	406994	ANU-ST57	Blood in EtOh	-80	720576	*Acanthornis magna magna*	12/04/2
Central North	406995	ANU-ST58	Blood in EtOh	-80	720576	*Acanthornis magna magna*	12/04/2
Central North	406996	ANU-ST59	Blood in EtOh	-80	720576	*Acanthornis magna magna*	12/04/2
Central North	406997	ANU-ST60	Blood in EtOh	-80	720576	*Acanthornis magna magna*	12/04/2
Central West	406998	ANU-ST61	Blood in EtOh	-80	720576	*Acanthornis magna magna*	13/04/2
Central West	406999	ANU-ST62	Blood in EtOh	-80	720576	*Acanthornis magna magna*	13/04/2
Central West	407000	ANU-ST63	Blood in EtOh	-80	720576	*Acanthornis magna magna*	13/04/2
Central West	407001	ANU-ST64	Blood in EtOh	-80	720576	*Acanthornis magna magna*	13/04/2
Central West	407002	ANU-ST65	Blood in EtOh	-80	720576	*Acanthornis magna magna*	13/04/2
Central West	407003	ANU-ST66	Blood in EtOh	-80	720576	*Acanthornis magna magna*	13/04/2
North East	406947	ANU-ST10	Blood in EtOh	-80	720576	*Acanthornis magna magna*	21/03/2
North East	406948	ANU-ST11	Blood in EtOh	-80	720576	*Acanthornis magna magna*	21/03/2
North East	406949	ANU-ST12	Blood in EtOh	-80	720576	*Acanthornis magna magna*	21/03/2
North East	406950	ANU-ST13	Blood in EtOh	-80	720576	*Acanthornis magna magna*	21/03/2
North East	406951	ANU-ST14	Blood in EtOh	-80	720576	*Acanthornis magna magna*	22/03/2

Source	Sample	Specimen	Tissue	Pres.	Taxon	Scientific name	Collecti
North East	406952	ANU-ST15	Blood in EtOh	-80	720576	*Acanthornis magna magna*	22/03/2
North East	406953	ANU-ST16	Blood in EtOh	-80	720576	*Acanthornis magna magna*	22/03/2
North East	407009	ANU-ST10	Blood in EtOh	-80	720576	*Acanthornis magna magna*	21/03/2
South Bruny Island	406938	ANU-ST01	Blood in EtOh	-80	720576	*Acanthornis magna magna*	14/03/2
South Bruny Island	406959	ANU-ST22	Blood in EtOh	-80	720576	*Acanthornis magna magna*	28/03/2
South Bruny Island	406960	ANU-ST23	Blood in EtOh	-80	720576	*Acanthornis magna magna*	28/03/2
South Bruny Island	406961	ANU-ST24	Blood in EtOh	-80	720576	*Acanthornis magna magna*	28/03/2
South East	406941	ANU-ST04	Blood in EtOh	-80	720576	*Acanthornis magna magna*	13/03/2
South East	406942	ANU-ST05	Feather in EtOh	-80	720576	*Acanthornis magna magna*	13/03/2
South East	406943	ANU-ST06	Blood in EtOh	-80	720576	*Acanthornis magna magna*	17/03/2
South East	406944	ANU-ST07	Blood in EtOh	-80	720576	*Acanthornis magna magna*	17/03/2
South East	406945	ANU-ST08	Blood in EtOh	-80	720576	*Acanthornis magna magna*	17/03/2
South East	406946	ANU-ST09	Feather in EtOh	-80	720576	*Acanthornis magna magna*	17/03/2
South East	406954	ANU-ST17	Blood in EtOh	-80	720576	*Acanthornis magna magna*	24/03/2
South East	406955	ANU-ST18	Blood in EtOh	-80	720576	*Acanthornis magna magna*	24/03/2
South East	406956	ANU-ST19	Blood in EtOh	-80	720576	*Acanthornis magna magna*	24/03/2
South East	406957	ANU-ST20	Blood in EtOh	-80	720576	*Acanthornis magna magna*	24/03/2
South East	406958	ANU-ST21	Blood in EtOh	-80	720576	*Acanthornis magna magna*	24/03/2
South East	407011	ANU-ST09	Feather in EtOh	-80	720576	*Acanthornis magna magna*	17/03/2
South West	406939	ANU-ST02	Blood in EtOh	-80	720576	*Acanthornis magna magna*	8/03/20
South West	406940	ANU-ST03	Blood in EtOh	-80	720576	*Acanthornis magna magna*	9/03/20
South West	407005	ANU-ST68	Blood in EtOh	-80	720576	*Acanthornis magna magna*	16/04/2
South West	407006	ANU-ST69	Blood in EtOh	-80	720576	*Acanthornis magna magna*	16/04/2
South West	407007	ANU-ST70	Blood in EtOh	-80	720576	*Acanthornis magna magna*	16/04/2
South West	407010	ANU-ST68	Blood in EtOh	-80	720576	*Acanthornis magna magna*	16/04/2
Tasman Peninsula	406962	ANU-ST25	Blood in EtOh	-80	720576	*Acanthornis magna magna*	1/04/20
Tasman Peninsula	406963	ANU-ST26	Blood in EtOh	-80	720576	*Acanthornis magna magna*	1/04/20
Tasman Peninsula	406964	ANU-ST27	Blood in EtOh	-80	720576	*Acanthornis magna magna*	1/04/20
Tasman Peninsula	406965	ANU-ST28	Blood in EtOh	-80	720576	*Acanthornis magna magna*	1/04/20
Tasman Peninsula	406966	ANU-ST29	Blood in EtOh	-80	720576	*Acanthornis magna magna*	1/04/20
Tasman Peninsula	406967	ANU-ST30	Blood in EtOh	-80	720576	*Acanthornis magna magna*	1/04/20
Tasman Peninsula	406968	ANU-ST31	Blood in EtOh	-80	720576	*Acanthornis magna magna*	1/04/20
Tasman Peninsula	406969	ANU-ST32	Blood in EtOh	-80	720576	*Acanthornis magna magna*	1/04/20
South Bruny Island	406970	ANU-ST33	Blood in EtOh	-80	720576	*Acanthornis magna magna*	5/04/20
South Bruny Island	406971	ANU-ST34	Blood in EtOh	-80	720576	*Acanthornis magna magna*	5/04/20
South Bruny Island	406972	ANU-ST35	Blood in EtOh	-80	720576	*Acanthornis magna magna*	5/04/20

Table S2: Summary of steps used to filter the VCF file in R.

Package	**Function**	**Criteria**
SNPfiltR	hard_filter	min depth = 5 min genotype quality = 20
	max_depth	max depth = 137 (i.e. 2*SD)
	min_mac	minimum minor allele count = 3
	filter_allele_balance	min ratio = 0.2 max ratio = 0.8
	filter_biallelic	keep biallelic SNPs only
Custom script		remove SNPs missing >5% data
		minimum minor allele count = 3
		retain SNPs with Ho < 0.6

Package	Function	Criteria
SNPRelate	snpgdsLDpruning	method="corr", ld.threshold = 0.5, slide.max.bp = 500000, autosome.only = FALSE
Custom script		Remove replicate samples and highly-related individuals
		Remove sex-linked loci
	tess3 & pvalue	Remove loci under putative selection
	gl.outflank	Remove loci under putative selection

Table S3: Genome assembly statistics of the Tasmanian scrubtit (*Acanthornis magna magna*).

Metric	
Assembly size (Gb)	1.48
Number of contigs	1,516
Contig N50 (Mb)	7.715
Contig L50	41
Contig N90 (Mb)	0.521
Contig L90	408
Longest contig (Mb)	60.595
GC content (%)	42.88
Complete BUSCOs	97.1% [Single copy: 96.4%; Duplicated: 0.7%]
Fragmented BUSCOs	0.5%
Missing BUSCOs	2.4%

Table S4: Classification of repeat elements of the Tasmanian scrubtit (*Acanthornis magna magna*) genome assembly.

Repeat element	Number of elements	% of sequence
SINEs	2,575	0.03
LINES LINE1	162,627 416 160,090	15.93 0 15.37
L3/CR1		
LTR elements ERVL	56,446 30,371 20,5402,917	7.79 4.89 2.65 0.16
ERV Class I		
ERV Class II		
DNA elements hAT-Charlie	17,631 118	0.58 0
Unclassified	133,829	6.18
Total interspersed repeats		30.52
Small RNA	958	0.06
Satellites	25,152	1.26

Table S5 : Pairwise F_{ST} values showing genetic differentiation between scrubtit subpopulations. Bootstrapped$p$ -value estimates above the are not known as all estimates were <.001. King Island scrubtit subpopulations shown in purple, Tasmanian scrubtit subpopulations shown in yellow.

		Central North	Central West	Colliers Swamp	Nook	North East	Pegarah	Bruny Is
PWF_{ST}	Central North							
	Central West	0.01						
	Colliers Swamp	0.2	0.22					

	Central North	Central West	Colliers Swamp	Nook	North East	Pegarah	Bruny Is
Nook	0.16	0.17	0.15				
North East	0.12	0.12	0.33	0.29			
Pegarah	0.18	0.2	0.18	0.12	0.31		
Bruny Island	0.09	0.08	0.28	0.24	0.18	0.26	
South East	0.03	0.01	0.21	0.17	0.12	0.18	0.07
South West	0.02	0.01	0.23	0.18	0.13	0.21	0.07
Tasman Peninsula	0.23	0.24	0.43	0.39	0.22	0.41	0.27

Table S6: Genetic diversity metrics for a-priori populations of King Island and Tasmanian scrubtits. Shown are mean subpopulation estimates ± the standard errors.

Region	**Locality**	**A**	$\mathbf{A_E}$	$\mathbf{H_E}$	$\mathbf{H_O}$	$\mathbf{F_{IS}}$	$\mathbf{II_C}$
King Island	Colliers Swamp	1.423 ± .007	1.258 ± .005	0.169 ± .003	0.170 ± .003	-0.009 ± .007	0.342 ±
	Nook	1.49 ± .007	1.302 ± .005	0.197 ± .003	0.200 ± .003	-0.014 ± .007	0.251 ±
	Pegarah	1.448 ± .007	1.277 ± .005	0.181 ± .003	0.166 ± .003	0.064 ± .008	0.365 ±
Mainland	Central North	1.816 ± .005	1.449 ± .004	0.282 ± .003	0.270 ± .003	0.038 ± .004	0.101 ±
	Central West	1.753 ± .006	1.439± .004	0.284 ± .003	0.270 ± .003	0.041 ± .005	0.093 ±
	North East	1.616 ± .007	1.343 ± .005	0.220 ± .003	0.216 ± .003	0.014 ± .005	0.196 ±
	South Bruny Island	1.671 ± .006	1.394 ± .005	0.251 ± .003	0.243 ± .003	0.026 ± .005	0.170 ±
	South East	1.838 ± .005	1.449 ± .005	0.282 ± .003	0.270 ± .003	0.037 ± .004	0.0779 ±
	South West	1.713 ± .006	1.426 ± .005	0.280 ± .003	0.268 ± .003	0.038 ± .006	0.085 ±
	Tasman Peninsula	1.448 ± .006	1.266 ± .0005	0.167 ± .003	0.163 ± .003	0.022 ± .006	0.354 ±

Table S7: Annotation of candidate SNPs associated with baldness. For SNPs in non-genic regions, the position and annotation of the closest gene upstream and downstream of the SNP are provided.

Genome contig	**Position of candidate SNP**	**Genic/non-genic**	**Position of gene or closest genes**	**Gene an**
ptg000013	11097938	Non-genic	11034629-11037505	*CALHM3*
			11137523-11196035	*NEURL1*
ptg000048	2661559	Genic	2551173-2690658	*GRIA3*, g
ptg000048	4113929	Genic	4091125-4123719	*DOCK11*
ptg000048	4025573	Non-genic	3933269-4012663	*TNIK*, T
			4025614-4034150	*MAP4K4*
ptg000272	649547	Non-genic	611019-613166	*MYH6,* n
			651350-652559	Unknown
ptg000602	69459	Genic	31541-121032	*NCOA1*,

Table S8: Effective population size estimates for the King Island and Tasmanian scrubtit and the respective a-priori subpopulations therein. Jackknifed estimates are derived from the 'no singleton alleles accepted' method in NeEstimator. 'Inf' denotes infinite estimate.

Population	**Subpopulation**	**Samples**	**Estimated Ne**	**Jackknifed estimate**
King Island		15	10	5 – 17
	Colliers Swamp	5	Inf	48 – inf
	The Nook	5	13.5	2 – inf
	Pegarah Forest	5	2.3	1 – 70

Population	Subpopulation	Samples	Estimated Ne	Jackknifed estimate
Mainland				
	East Coast	15	8	3 – 10
	Rest of mainland	40	137	56 – 113
	South East	11	48	12 – 132
	South West	5	Inf	Inf
	Central West	6	Inf	133 – Inf
	Central North	10	154	39 – 112
	South Bruny Island	7	954	68 – Inf
	North East	7	1587	Inf
	Tasman Peninsula	8	375	346 – inf

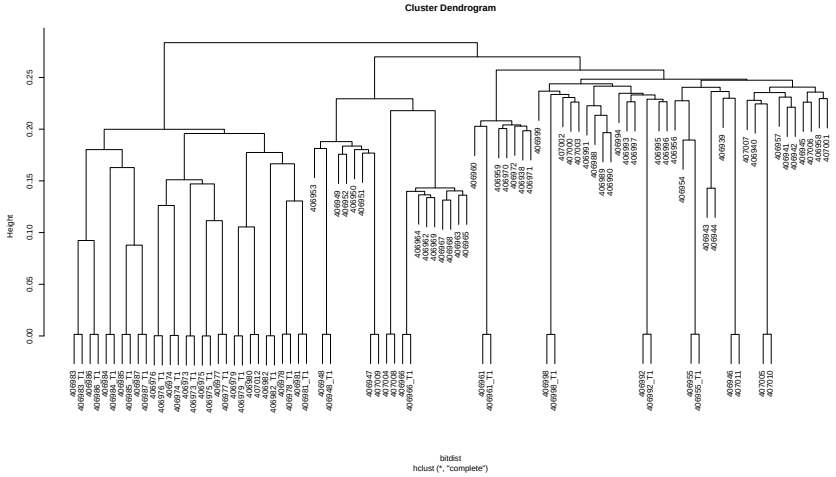

Figure S1a: Cluster dendrogram showing the bitwise genetic distance between scrubtit samples. Branch labels correspond to the bioplatforms library ID, the dual library index ID and the library index sequence. Labels with R- denote technical replicates. Tight pairs on long branches denote replicated samples, note however that not all replicates are labelled as technical replicates.

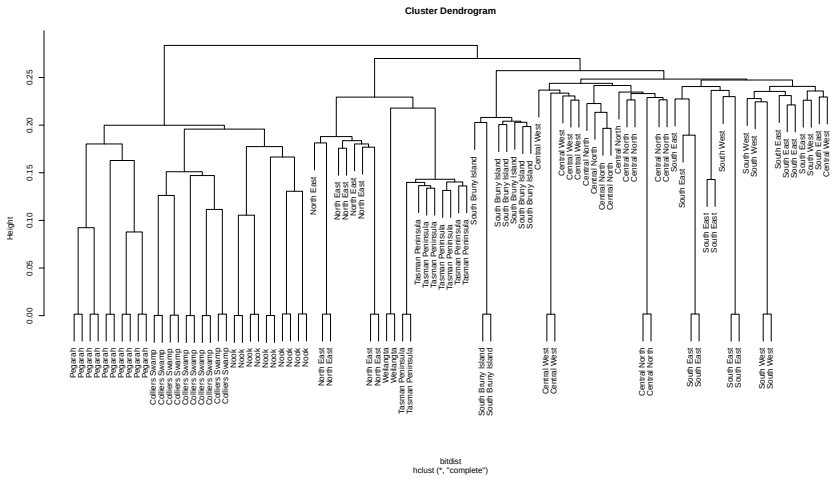

Figure S1b : Cluster dendrogram showing the bitwise genetic distance between scrubtit samples. Branch labels correspond to the sampling locations. Tight pairs on long branches denote replicated samples as shown in Figure S1a.

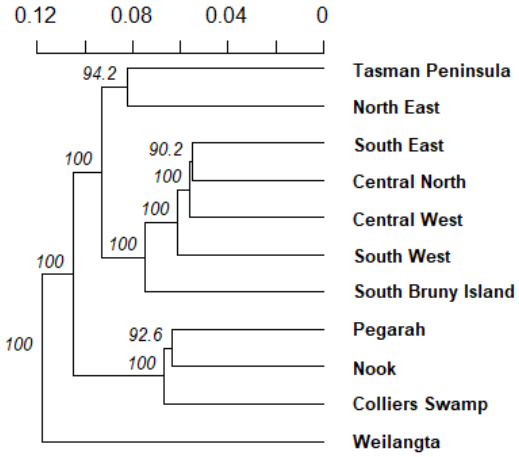

Figure S2: Bootstrapped dendrogram showing subpopulation-level differentiation in the King Island and Tasmanian scrubtit. Values on branches denote bootstrapped probability estimates. Weilangta population was just a single sample, so the position of that population is likely to change with additional samples from that locality.

Figure S3: Images of pattern baldness in affected King Island scrubtits.

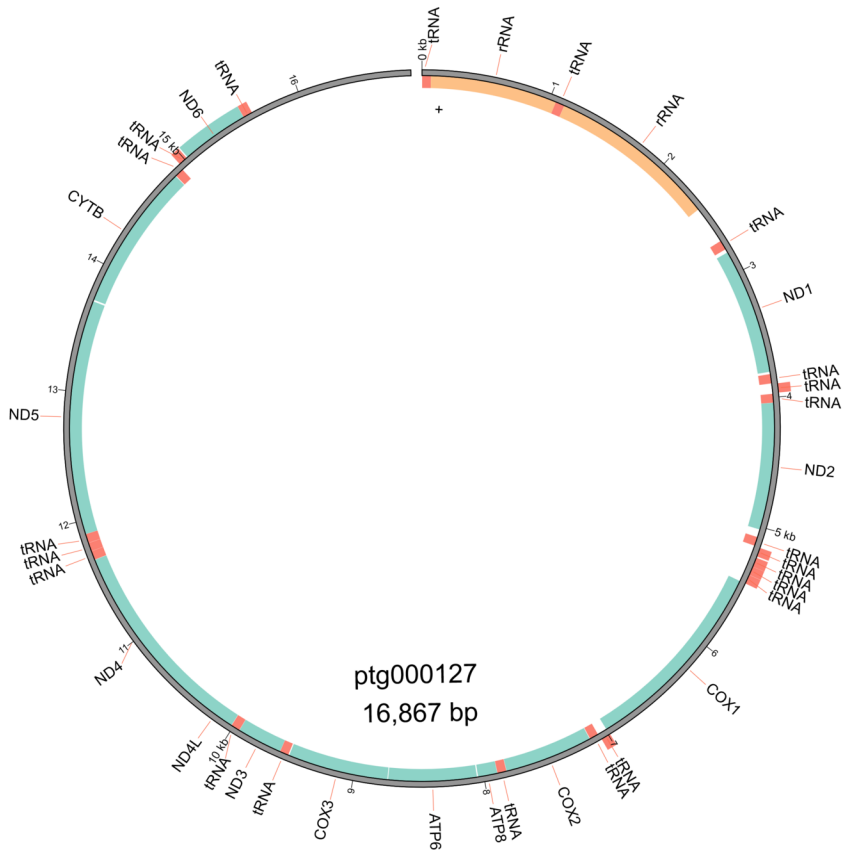

Figure S4: Mitochondrial genome of the King Island scrubtit (*Acanthornis magna greeniana*).

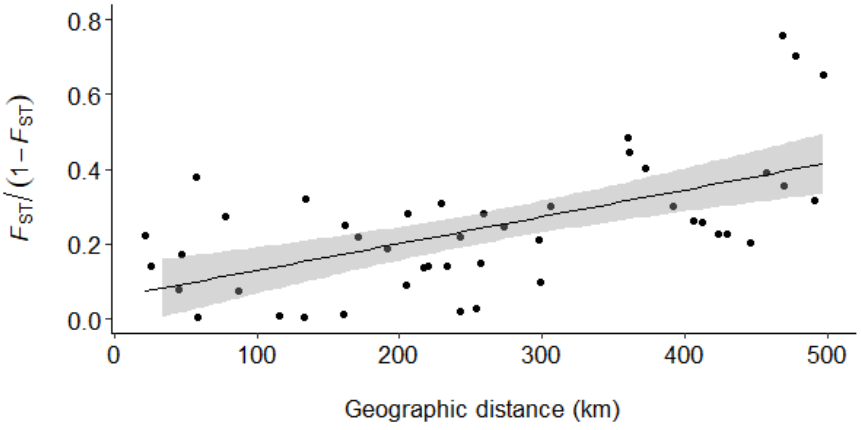

Figure S5: Standardized relationship between geographic distance and individual-level genetic differentiation in King Island and Tasmanian scrubtits. Prediction is derived from a linear model, shading represents 95% confidence interval.

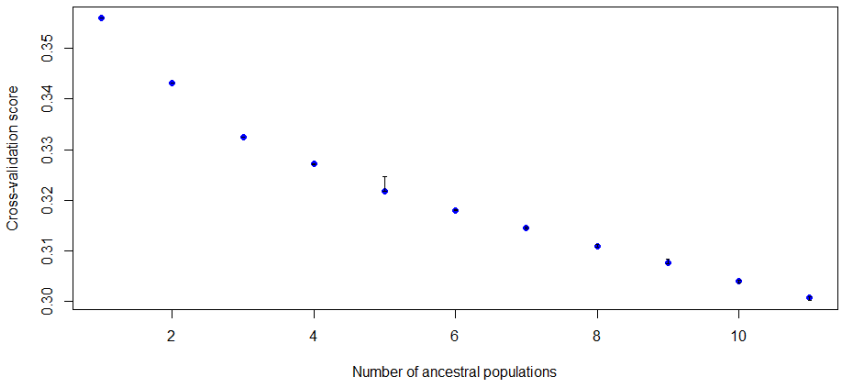

Figure S6: Cross-entropy plot used to identify hierarchical population structuring in the genomic dataset for King Island and Tasmanian scrubtits. Lower values of the cross-entropy criterion indicate a better fit to the data. The relatively large drops in cross-entropy scores between 1 and 2, 2 and 3 and (to a lesser extent) between 3 and 4 ancestral populations (k) indicates that $k$values of 2, 3 or 4 are well-supported, although higher levels of$k$ further subdivide *a-priori* populations into clusters that correspond with the spatial pattern of sampling.

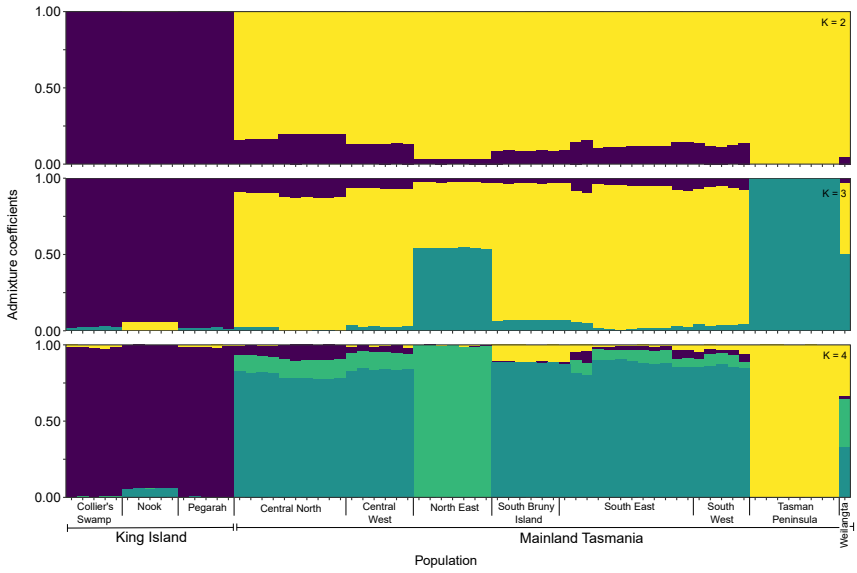

Figure 1:

Figure S7 : Admixture plots showing the probability assignment of each individual scrubtit to a-priori subpopulations based on sampling locations when the number of ancestral populations (k) ranged from 2 to 4.

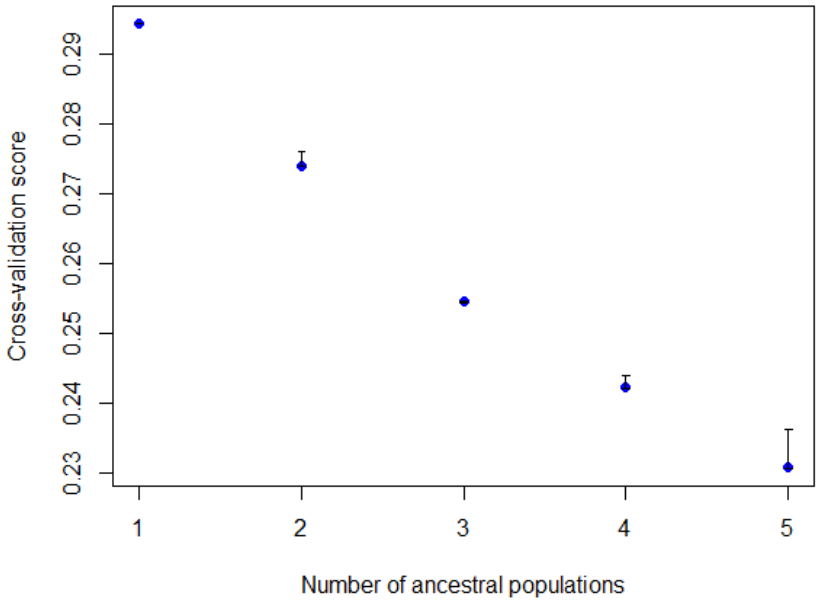

Figure S8: Cross-entropy plot used to identify hierarchical population structuring in the genomic dataset for King Island scrubtits. Lower values of the cross-entropy criterion indicate a better fit to the data. The relatively large drops in cross-entropy scores between 1 and 2, 2 and 3 ancestral populations (k) indicates that $k$values of 2 and 3 are well-supported.

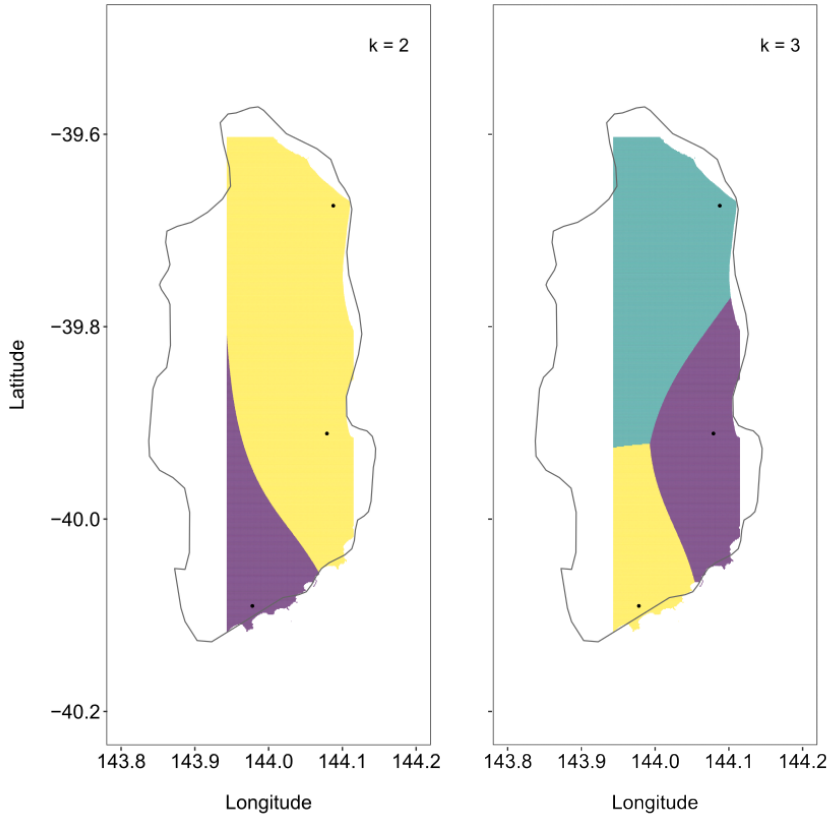

Figure S9: Patterns of landscape genomic structure in the King Island scrubtit. Panels show the population genomic structure when two and three ancestral clusters (k values) are identified in the data set. Colours in each panel represent the distribution of an ancestral cluster, interpolated across King Island. Black points indicate sampling locations.

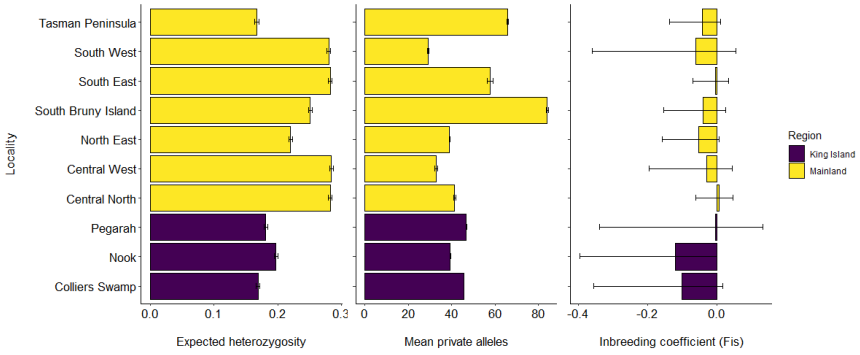

Figure S10: Estimates of genetic diversity (H_E& P_A) and inbreeding (F_{IS}) across Tasmanian scrubtit and King Island scrubtit subpopulations. Error bars show standard errors for H_E and P_A, and 95 % confidence intervals for F_{IS}.

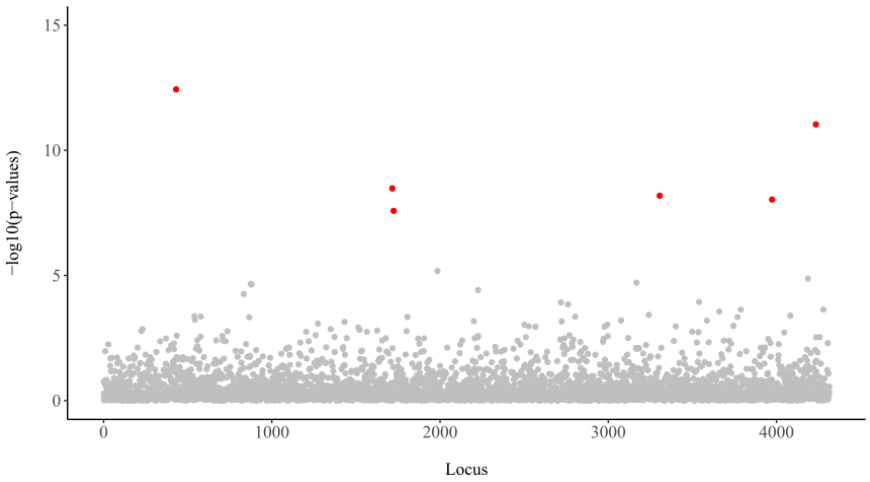

Figure S11: Manhattan plot showing the probability of a SNP showing an association with pattern baldness in King Island scrubtits by locus position. The six outlier loci with small p- values are shown in red.